PB86-110996

SEISMIC WATER PRESSURES ON DAMS FOR ARBITRARILY SHAPED RESERVOIRS

by

Long-Cheng Huang and Allen T. Chwang

Partially sponsored by
National Science Foundation
Grant CEE-8020564 A01

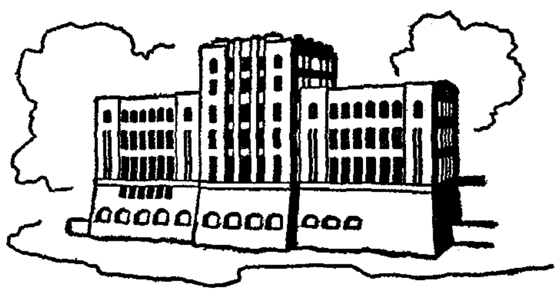

IIHR Report No. 291

Iowa Institute of Hydraulic Research
The University of Iowa
Iowa City, Iowa 52242

September 1985

SEISMIC WATER PRESSURES ON DAMS FOR ARBITRARILY SHAPED RESERVOIRS

by

Long-Cheng Huang and Allen T. Chwang

Partially sponsored by
National Science Foundation
Grant CEE-8020564 A01

IIHR Report No. 291

Iowa Institute of Hydraulic Research
The University of Iowa
Iowa City, Iowa 52242

September 1985

ABSTRACT

This report represents essentially the thesis submitted by Long-Cheng Huang in partial fulfillment of the requirements for the degree of Doctor of Philosophy in Civil and Environmental Engineering at The University of Iowa. Professor Allen T. Chwang was supervisor of the research project and thesis advisor.

An accurate hydrodynamic pressure distribution on the vertical upstream face of a flexible dam due to ground excitations is obtained, by analytical and numerical methods, for a three-dimensional, arbitrarily shaped reservoir with a rigid vertical side boundary.

The solution for the velocity potential is expressed analytically in terms of a set of line integrals along the reservoir boundary. These integrals are then converted into a matrix equation with the boundary being divided into a sufficiently large number of segments and the average value of the velocity potential along each segment is used to represent that segment. The matrix equation is solved numerically and the hydrodynamic pressure distribution on the dam-reservoir interface is determined in terms of the velocity potential through the Bernoulli equation. An integration of the hydrodynamic pressure distribution yields the total earthquake loading on a dam.

The effect of the surface waves and the compressibility effect of water on seismic water pressures have been studied in detail. The present results are in good agreement with the analytical solutions derived by Huang and

Chwang (1982) and Kadle and Chwang (1982) when the reservoir has a simple geometric shape such as a rectangle, a circle, or a semi-circle in the rigid dam case. By expressing the deformation of a dam at the interface of the coupled dam-reservoir system as a linear combination of the first four mode shapes of the dam itself, the effect of the dam flexibility is briefly discussed. It is found that the compressibility of water and the flexibility of a dam change significantly the hydrodynamic pressure forces acting on the dam.

TABLE OF CONTENTS

LIST OF FIGURES

LIST OF SYMBOLS

$A(x,y)$	attenuation function
a	amplitude of ground motion
B	dimensionless compressibility parameter $\omega h/c_o$
b	width of dam
$[C]$	damping matrix of a dam
C	dimensionless wave-effect parameter $g/\omega^2 h$
C_f	dimensionless force coefficient
C_{fi}	in-phase component of the dimensionless force coefficient
C_{fo}	out-of-phase component of the dimensionless force coefficient
C_m	dimensionless moment coefficient
C_{mi}	in-phase component of the dimensionless moment coefficient
C_{mo}	out-of-phase component of the dimensionless moment coefficient
C_p	dimensionless pressure coefficient
C_{pi}	in-phase component of the dimensionless pressure coefficient
C_{po}	out-of-phase component of the dimensionless pressure coefficient
c_o	speed of sound in water

D	plate flexural rigidity
d	thickness of dam
E	Young's modulus of elasticity
$\underline{F}$	applied force vector on dam
f_j	jth normal-mode shape of dam
G, G_n	matrices defined in equation 3.6
G_o	$k_o h\ Q_o(1-C) + 1$
G_m	$k_m h\ Q_m(1-C) - 1$
g	gravitational constant
H	height of dam
$H_n^{(1)}$	Hankel function of first kind, of order n
h	constant depth of reservoir
J_n	Bessel function of first kind, of order n
[K]	stiffness matrix of a dam
K_n	modified Bessel function of second kind, of order n
k_o	root of $Ck_o h \tanh (k_o h) - 1 = 0$
k_m	roots of $Ck_m h \tan (k_m h) + 1 = 0$
ℓ	length of rectangular reservoir
M	largest integer for which $k_m \leq \frac{\omega}{c_o}$
[M]	mass matrix of a dam
m	mass per unit area of a plate dam
N	segments number into which the boundary is divided
P	hydrodynamic pressure
Q_o	$\sinh (k_o h)$
Q_m	$\sin (k_m h)$

R	radius of circular and semi-circular reservoir
r	radial distance of semi-circular reservoir
S	mass ratio of water to dam $\rho_0 h/m$
t	time
T	period of ground motion
U, U_n	matrices defined in equation 3.9
$\underline{W}$, $\underline{X}$, $\underline{Y}$, $\underline{Z}$	vectors defined in equations 3.6 and 3.9
Y_j	jth-mode generalized coordinate of dam
∂D	boundary of arbitrarily shaped reservoir
α	interior angle of pointed boundary
β_m	$\sqrt{k_m^2 - (\frac{\omega}{c_0})^2}$
Δ	definition defined in equation 2.3
ε	radius of small circle (Fig. A.1)
ζ	displacement of a dam
η	water surface profile
θ_f	phase difference between the in-phase and out-of-phase component of the force coefficient
θ_m	phase difference between the in-phase and out-of-phase component of the moment coefficient
θ_p	phase difference between the in-phase and out-of-phase component of the pressure coefficient
λ_j^2	dimensionless eigenvalues $b^2 \omega_j \sqrt{\frac{m}{D}}$
μ_0	$\sqrt{(\frac{\omega}{c_0})^2 + k_0^2}$

μ_m	$\sqrt{(\frac{\omega}{c_o})^2 - k_m^2}$
ν	Poisson's ratio of plate material
ξ_j	jth-mode damping ratio
ρ_o	undisturbed water density
ϕ	velocity potential
ψ	solutions of Helmholtz equation
ω	frequency of ground motion
ω_j	the jth-mode natural frequency of a dam
*	superscript denotes the complex frequency response
j	subscript denotes the jth-mode vibration

CHAPTER I

INTRODUCTION

1.1. Review of Pertinent Literature

During an earthquake, a dam accelerates into and away from the reservoir, and as a result develops a hydrodynamic pressure in excess of the hydrostatic pressure. Depending on the intensity of the ground excitation, this pressure can be large enough to cause damage to a dam. In view of the disastrous consequences of a dam failure during an earthquake, it is necessary to develop an adequate analytical method to study the earthquake effect on a dam-reservoir system.

For an infinitely long reservoir, Westergaard (1933) first derived an expression for the hydrodynamic pressure exerted on a rigid dam with a vertical upstream face by an incompressible fluid in the reservoir. The "added mass" theory was presented in his paper by ignoring the effect of surface waves.

Since the pioneering work of Westergaard, a series of investigations have been conducted to study the seismic response of rigid dam-reservoir systems for incompressible and compressible water. Kotsubo (1959, 1961) obtained a general solution for both transient and steady-state hydrodynamic pressures acting on a rigid concrete dam. Chopra (1967) demonstrated that the hydrodynamic response of a compressible fluid during an earthquake is different from that of an incompressible fluid.

For a dam whose upstream face is not vertical, Zanger (1953) and Zanger and Haefeli (1952) determined the hydrodynamic pressures experimentally using an electrical analogue. They concluded that the hydrodynamic pressure on a dam with the upstream face vertical for more than half of the total height would practically be the same as that of a fully vertical dam. Recently, Chwang and Housner (1978) and Chwang (1978) found that the normal-force coefficient remains practically constant at around 0.5 for all slopes.

The effect of a finite reservoir on the hydrodynamic pressure was investigated by Werner and Sundquist (1946) and by Chwang (1979). Chwang (1979) found that for horizontal accelerations the hydrodynamic pressure force decreases as the size of the reservoir decreases. He also found that the effect of vertical acceleration on the pressure force exerted on a dam is simply to adjust the hydrostatic pressure by replacing the gravitational constant by an effective gravitational acceleration if the fluid in the reservoir is incompressible, and this is true for any arbitrarily shaped reservoir. The possibility of cavitation at some point on the upstream face of a dam has been discussed, and the effect of non-horizontal bottom has also been studied.

The effect of fluid stratification in the reservoir on hydrodynamic pressure was analyzed by Chwang (1981), who also discussed the effect of surface waves.

A series of papers by Chopra (1968, 1970) and Chakrabarti and Chopra (1973a, 1973b, 1974) revealed that the elasticity and flexibility of a dam have also profound effects on the hydrodynamic pressures. In these papers, the deformation of the interface of the coupled dam-reservoir system was expressed as a linear combination of the normal modes of vibration of the dam itself.

All the aforementioned papers treated the dam-reservoir system as a two-dimensional problem, considering only the planar vibration of a linearly elastic dam cross-section without taking into account the abutment and the side confinement of the reservoir which, in reality, can be expected to affect the hydrodynamic pressures considerably. Therefore the two-dimensional analysis appears to be an approach that is too over-simplified to predict accurately the dynamic behavior of a three-dimensional coupled dam-reservoir system.

Three-dimensional rectangular dam-reservoir systems with vertical side-boundaries were analyzed by Huang and Chwang (1982). Both longitudinal and lateral harmonic excitations were investigated, and the effect of compressibility of water, seismic wave attenuation, phase difference between two ends of a reservoir, and the possibility of resonance were also discussed. The effects of the seismic attenuation and the phase difference were found to be small. Kadle and Chwang (1982) investigated the three-dimensional circular and semicircular dam-reservoir systems, the effects of surface waves were discussed in detail and the resonances were found to occur when the ratio of the fluid depth to the period of the ground motion was greater than 360 m/sec. In both papers, the dam was assumed to be rigid.

1.2. Outlines and Assumptions

The present work is concerned with the boundary irregularity effect on seismic water pressures on dams during earthquakes, including the compressibility and the surface wave effects of the fluid and the flexibility effect of the dam. The hydrodynamic pressure is the real part of the complex pressure due to a horizontal acceleration, $ae^{-i\omega t}$, in the x or y direction.

The following assumptions are made in this study:

(1) The fluid is compressible and inviscid and the flow is irrotational with the presence of surface waves.

(2) The upstream face of a dam is vertical.

(3) The reservoir bottom is horizontal and the side boundary is vertical and rigid.

(4) There is no density stratification of the fluid in the reservoir.

(5) The amplitude of the excitation is small.

By analytical and numerical methods, the velocity potential can be expressed in terms of a set of line integrals along the boundary, and so can the hydrodynamic pressure. The effects of surface waves and the compressibility of water are included in this study. The results obtained are checked with the existing theoretical solutions for reservoirs with simple shapes. By expressing the deformation of a dam as a linear combination of the first four mode shapes of the dam itself, the flexibility effect of the dam is also investigated.

CHAPTER II

THEORETICAL ANALYSIS

2.1. Governing Equations and Boundary Conditions

We shall analyze a dam-reservoir system in which the reservoir is arbitrary in shape with a constant depth h and vertical side boundary, and the vertical dam has a constant width b, and height H.

Let the coordinate origin be located at the center of the base of the dam. The x-axis is in the direction perpendicular to the upstream face of the dam and lies in the horizontal ground plane. The y-axis is perpendicular to the x-axis in the horizontal plane, and the z-axis is pointing vertically upwards. The bottom of the reservoir is at $z = 0$. The profile of free surface is denoted by $z = h + \eta(x,y,t)$. The arbitrarily shaped reservoir is bounded by ∂D, and the upstream face of the dam which is located at $x = 0$, extending from $y = -b/2$ to $b/2$ (see Fig. 1).

It is assumed that the ground acceleration is $ae^{-i\omega t}$ along the positive x (longitudinal) or the positive y (lateral) direction.

2.1.1. Dam

The motion of the flexible dam is governed by

$$[M]\,\ddot{\underline{\zeta}} + [C]\,\dot{\underline{\zeta}} + [K]\,\underline{\zeta} = \underline{F}, \tag{2.1}$$

where $\underline{\zeta}(x,y,z,t)$ is the displacement vector, [M] the mass matrix, [C] the damping matrix, [K] the stiffness matrix and $\underline{F}$ the applied external force vector which includes the normal hydrodynamic pressure force and the ground acceleration force at the base and on the side boundaries due to an earthquake.

The displacement of the upstream face of the dam in the x direction, relative to the base, can be expressed as a linear combination of its normal-mode shapes

$$\zeta(y,z,t) = \sum_{j=1}^{\infty} Y_j(t)\, f_j\,(y,z), \tag{2.2}$$

where $Y_j(t)$ is the generalized coordinate and $f_j(y,z)$ is the normal-mode shape for the jth mode of the dam. In reality, only the first few modes (say, J modes) of the dam are important.

The boundary conditions on $\zeta(y,z,t)$ for a flexible dam are as follows:

(i) The dam is clamped at the bottom ($z = 0$) and at two sides ($y = \pm\, b/2$). Therefore, the displacement ζ and its normal derivative must vanish at the clamped boundary.

(ii) The dam is free at the top ($z = H$). Hence, the shear stress and the moment must vanish at $z = H$.

The total acceleration in the x direction on the dam-reservoir interface due to a ground acceleration $ae^{-i\omega t}$ at the base of the dam is

$$\ddot{\zeta}(y,z,t) = \Delta a e^{-i\omega t} + \sum_{j=1}^{J} \ddot{Y}_j(t)\, f_j(y,z), \tag{2.3}$$

where dot denotes differentiation with respect to the time t, $\Delta = 1$ when the acceleration is in the x direction and $\Delta = 0$ when the acceleration is in the y direction. For a harmonic ground excitation, the generalized acceleration response for the dam is of the form

$$\ddot{Y}_j(t) = \ddot{Y}_j^*(\omega)\, e^{-i\omega t}, \tag{2.4}$$

where $\ddot{Y}_j^*(\omega)$ is the complex frequency response of $\ddot{Y}_j(t)$. Substituting (2.4) into (2.3), we have

$$\ddot{\zeta}(y,z,t) = [\Delta a + \sum_{j=1}^{J} \ddot{Y}_j^*(\omega)\, f_j(y,z)]e^{-i\omega t}. \tag{2.5}$$

2.1.2. Reservoir

For inviscid, irrotational motions of compressible water in a reservoir, the velocity vector has a scalar potential ϕ. If the motion of the water is assumed to be small in amplitude, the equation of motion for the water is the wave equation

$$\frac{\partial^2 \phi}{\partial x^2} + \frac{\partial^2 \phi}{\partial y^2} + \frac{\partial^2 \phi}{\partial z^2} = \frac{1}{c_0^2} \frac{\partial^2 \phi}{\partial t^2}, \tag{2.6}$$

where $\phi(x,y,z,t)$ is the velocity potential and c_0 is the speed of sound in water. The hydrodynamic pressure $P(x,y,z,t)$ is related to ϕ by

$$P = -\rho_0 \frac{\partial \phi}{\partial t} \tag{2.7}$$

where ρ_0 is the undisturbed density of water.

The boundary conditions for ϕ subjected to an acceleration of $ae^{-i\omega t}$ are as follows:

(i) Normal velocity at the bottom of the reservoir must vanish:

$$\frac{\partial \phi}{\partial z}(x,y,0,t) = 0. \tag{2.8}$$

(ii) Normal velocities of the fluid on the upstream face of the dam ($x = 0$) and on reservoir boundary ∂D must be the same as those of the solid:

$$\frac{\partial\phi}{\partial x}(0,y,z,t) = \frac{i}{\omega}\left[\Delta a + \sum_{j=1}^{J} \ddot{Y}_j^*(\omega)\, f_j(y,z)\right]e^{-i\omega t}, \qquad (2.9)$$

$$\frac{\partial\phi}{\partial n}(x,y,z,t) = a\,\frac{i}{\omega}\,A(x,y)\;e^{-i\omega t} \text{ on } \partial D, \qquad (2.10)$$

where $A(x,y)$ is an attenuation function, and $\partial/\partial n$ denotes the normal derivative.

(iii) The linearized kinematic boundary condition at the free surface is

$$\frac{\partial\eta}{\partial t}(x,y,t) - \frac{\partial\phi}{\partial z}(x,y,h,t) = 0 \text{ at } z = h. \qquad (2.11)$$

(iv) The linearized dynamic boundary condition at the free surface is

$$\frac{\partial\phi}{\partial t}(x,y,h,t) + g\eta(x,y,t) = 0 \quad \text{at } z = h, \qquad (2.12)$$

where g is the gravitational constant.

Combining (2.11) and (2.12), we obtain the free-surface boundary condition

$$\frac{\partial^2\phi}{\partial t^2} + g\,\frac{\partial\phi}{\partial z} = 0 \qquad \text{at } z = h. \qquad (2.13)$$

Let $\phi(x,y,z,t) = \phi_0(x,y,z,t) + \sum_{j=1}^{J} \frac{\ddot{Y}_j^*(\omega)}{a} \phi_j(x,y,z,t)$, where ϕ_j satisfies the governing equation

$$\frac{\partial^2\phi_j}{\partial x^2} + \frac{\partial^2\phi_j}{\partial y^2} + \frac{\partial^2\phi_j}{\partial z^2} = \frac{1}{c_0^2}\frac{\partial^2\phi_j}{\partial t^2} \; (j = 0,1,2,\ldots J). \tag{2.14}$$

ϕ_0 satisfies the boundary conditions (2.8), (2.10), (2.13) and

$$\frac{\partial\phi_0}{\partial x}(0,y,z,t) = \frac{i}{\omega}\Delta a e^{-i\omega t} \qquad \text{on the dam.} \tag{2.15}$$

ϕ_j satisfies the boundary conditions (2.8), (2.13) and

$$\frac{\partial\phi_j}{\partial x}(0,y,z,t) = \frac{i}{\omega}\, a\, f_j(y,z)\, e^{-i\omega t} \quad \text{on the dam,} \tag{2.16}$$

$$\frac{\partial\phi_j}{\partial n}(x,y,z,t) = 0 \qquad \text{on } \partial D. \tag{2.17}$$

2.2. Velocity Potential

The solution of (2.14), subject to the boundary conditions (2.15) to (2.17), can be obtained by the method of separation of variables as

$$\phi_j(x,y,z,t) = a\,\frac{i}{\omega}\, e^{-i\omega t}\, [\psi_{j0}(x,y) \cosh(k_0 z)$$

$$+ \sum_{m=1}^{\infty} \psi_{jm}(x,y) \cos(k_m z)]$$

$$(j = 0,1,2,\ldots J), \tag{2.18}$$

where k_o satisfies the dispersion relation

$$\omega^2 = gk_o \tanh(k_o h), \tag{2.19}$$

or

$$1 - C\,k_o h \tanh(k_o h) = 0, \tag{2.20}$$

and k_m satisfies

$$1 + C\,k_m h \tan(k_m h) = 0, \tag{2.21}$$

and the wave-effect parameter C (Chwang, 1981) is given by

$$C = \frac{g}{\omega^2 h}. \tag{2.22}$$

In equation (2.18), $\psi_{jo}(x,y)$ satisfies

$$\nabla^2\psi_{jo} + \mu_o^2\,\psi_{jo} = 0, \tag{2.23a}$$

where ∇^2 is the two-dimensional Laplacian operator in the x-y space and

$$\mu_o = \sqrt{\left(\frac{\omega}{c_o}\right)^2 + k_o^2}\ . \tag{2.23b}$$

An alternate form of equation (2.23b) is

$$\mu_o h = (B^2 + k_o^2 h^2)^{1/2},$$

where

$$B = \omega h/c_o \tag{2.23c}$$

is a dimensionless parameter, which measures the compressibility effect of water. $B = 0$ means the water is treated as incompressible. The boundary conditions for ψ_{oo} are

$$\left.\frac{\partial\psi_{oo}}{\partial x}\right|_{x=0} = \frac{2\Delta}{k_o h}\,\frac{Q_o}{1+CQ_o^{\,2}} \quad \text{on the dam,} \tag{2.23d}$$

$$\frac{\partial\psi_{oo}}{\partial n} = \frac{2}{k_o h}\,A(x,y)\,\frac{Q_o}{1+CQ_o^{\,2}} \quad \text{on } \partial D, \tag{2.23e}$$

and for $\psi_{jo}(j=1,2,\ldots J)$ are

$$\left.\frac{\partial\psi_{jo}}{\partial x}\right|_{x=0} = \frac{2}{h(1+CQ_o^{\,2})}\int_0^h f_j(y,z)\cosh(k_o z)\,dz \text{ on the dam,} \tag{2.23f}$$

$$\frac{\partial\psi_{jo}}{\partial n} = 0 \qquad \text{on } \partial D, \tag{2.23g}$$

where

$$Q_o = \sinh(k_o h). \tag{2.23h}$$

Let M be the largest integer such that $k_m \leq \omega/c_o$. Then for $m \leq M$, $\psi_{jm}(x,y)$ satisfies

$$\nabla^2\psi_{jm} + \mu_m^2\,\psi_{jm} = 0 \qquad (m \le M), \tag{2.24a}$$

where

$$\mu_m = \sqrt{\left(\frac{\omega}{c_o}\right)^2 - k_m^2}. \tag{2.24b}$$

When $k_m = \omega/c_o$, resonance occurs (see Kadle and Chwang, 1982). For $m>M$, $\psi_{jm}(x,y)$ is a solution of

$$\nabla^2\psi_{jm} - \beta_m^2\,\psi_{jm} = 0 \qquad (m > M), \tag{2.25a}$$

where

$$\beta_m = \sqrt{k_m^2 - \left(\frac{\omega}{c_o}\right)^2}. \tag{2.25b}$$

The boundary conditions to be satisfied by ψ_{jm}'s are

$$\left.\frac{\partial\psi_{om}}{\partial x}\right|_{x=0} = \frac{2\Delta}{k_m h}\,\frac{Q_m}{1-CQ_m^2} \qquad \text{on the dam,} \tag{2.26a}$$

$$\frac{\partial\psi_{om}}{\partial n} = \frac{2}{k_m h}\,A(x,y)\,\frac{Q_m}{1-CQ_m^2} \qquad \text{on } \partial D, \tag{2.26b}$$

and

$$\left.\frac{\partial\psi_{jm}}{\partial x}\right|_{x=0} = \frac{2}{h(1-CQ_m^2)}\int_0^h f_j(y,z)\cos(k_m z)\,dz \qquad \text{on the dam,} \tag{2.26c}$$

$$\frac{\partial\psi_{jm}}{\partial n} = 0 \qquad \text{on } \partial D, \tag{2.26d}$$

where

$$Q_m = \sin(k_m h). \tag{2.26e}$$

Hence $\phi(x,y,z,t)$ can be obtained in terms of the functions $\psi_{jm}(x,y)$ ($j = 0,1,2,\ldots J$ and $m = 0,1,2,3,\ldots$) which can be determined numerically for an arbitrarily shaped reservoir, as is discussed in the next chapter.

If there are no surface gravity waves (i.e. $C = 0$), (2.18) reduces to

$$\phi_j(x,y,z,t) = a\,\frac{i}{\omega}\,e^{-i\omega t}\,[\sum_{m=1}^{\infty}\psi_{jm}(x,y)\cos(k_m z)]$$

$$(j = 0,1,2,\ldots J), \qquad (2.27)$$

where $k_m = \dfrac{(2m-1)\pi}{2h}$.

2.3. Hydrodynamic Pressure Distribution

Since the governing equations and the boundary conditions are linear, the principle of superposition applies. The hydrodynamic pressure $P(x,y,z,t)$ due to harmonic ground motion can be expressed as

$$P(x,y,z,t) = P_o(x,y,z,t) + \sum_{j=1}^{J}\frac{\ddot{Y}_j^*(\omega)}{a}\,P_j(x,y,z,t). \qquad (2.27)$$

We note that $P_o(x,y,z,t)$ is the hydrodynamic pressure for a rigid dam, and $P_j(x,y,z,t)$ corresponds to the pressure for the jth mode of vibration with the base of the dam being fixed.

The hydrodynamic pressure at the dam face can be obtained as the real part of (2.7) at $x = 0$. Therefore, by (2.7) and (2.18), $P_j(0,y,z,t)$ $(j = 0,1,2,\ldots J)$ is

$$P_j(0,y,z,t) = \mathrm{Re}\,\{-\rho_o a e^{-i\omega t}[\psi_{jo}(0,y)\cosh(k_o z) + \sum_{m=1}^{\infty} \psi_{jm}(0,y)\cos(k_m z)]\}, \tag{2.28}$$

where Re denotes the real part.

The hydrodynamic-pressure distribution on the dam, normalized with respect to $\rho_o ah$, is

$$\frac{P(0,y,z,t)}{\rho_o ah} = C_{pi}\cos\omega t + C_{po}\sin\omega t, \tag{2.29a}$$

where the in-phase pressure coefficient C_{pi} is given by (2.27) and (2.28) as

$$C_{pi} = C_{pi}^{o} + \sum_{j=1}^{J} \frac{\ddot{Y}_j^{*}(\omega)}{a} C_{pi}^{j}, \tag{2.29b}$$

in which

$$C_{pi}^{j} = -\frac{1}{h}\,\mathrm{Re}\,\{\psi_{jo}(0,y)\cosh(k_o z) + \sum_{m=1}^{\infty} \psi_{jm}(0,y)\cos(k_m z)\}$$

$$(j = 0,1,2,\ldots J), \tag{2.29c}$$

and the out-of-phase pressure coefficient C_{po} is given by

$$C_{po} = C_{po}^{o} + \sum_{j=1}^{J} \frac{\ddot{Y}_j^*(\omega)}{a} C_{pi}^{j}, \tag{2.29d}$$

in which

$$C_{po}^{j} = -\frac{1}{h} I_m\{\psi_{jo}(0,y) \cosh (k_o z) + \sum_{m=1}^{\infty} \psi_{jm}(0,y) \cos (k_m z)\}$$

$$(j = 0,1,2,\ldots J), \tag{2.29e}$$

where Im denotes the imaginary part. Alternatively, the dimensionless pressure distribution on the dam may be expressed as

$$C_{pi} \cos \omega t + C_{po} \sin \omega t = C_p \cos (\omega t - \theta_p), \tag{2.29f}$$

where

$$C_p = (C_{pi}^2 + C_{po}^2)^{1/2}, \; \theta_p = \tan^{-1}(C_{po}/C_{pi}). \tag{2.29g}$$

2.4. Force and Moment Coefficients

The hydrodynamic pressure force acting on the dam, normalized with respect to $\rho_o a h^2$, is obtained by integrating (2.29) with respect to z from z = 0 to z = h. Hence, we have the dimensionless force coefficients as

$$C_{fi} \cos \omega t + C_{fo} \sin \omega t = C_f \cos (\omega t - \theta_f), \tag{2.30a}$$

where

$$C_f = (C_{fi}{}^2 + C_{fo}{}^2)^{1/2}, \ \theta_f = (C_{fo}/C_{fi}), \tag{2.30b}$$

$$C_{fi} = C_{fi}{}^{0} + \sum_{j=0}^{J} \frac{\ddot{Y}_j^*(\omega)}{a} C_{fi}{}^{j}, \tag{2.30c}$$

$$C_{fo} = C_{fo}{}^{0} + \sum_{j=0}^{J} \frac{\ddot{Y}_j^*(\omega)}{a} C_{fo}{}^{j}, \tag{2.30d}$$

$$C_{fi}^{j} = -\frac{1}{h} \mathrm{Re} \{\frac{Q_o}{k_m h} \psi_{jo}(0,y) + \sum_{m=1}^{\infty} \frac{Q_m}{k_m h} \psi_{jm}(0,y)\}, \tag{2.30e}$$

$$C_{fo}^{j} = -\frac{1}{h} \mathrm{Im}\{\frac{Q_o}{k_o h} \psi_{jo} (0,y) + \sum_{m=1}^{\infty} \frac{Q_m}{k_m h} \psi_{jm}(0,y)\} \ (j = 0,1,2,...J). \tag{2.30f}$$

In general, C_f is a function of y. The total force coefficient can be obtained by integrating (2.30) with respect to y from $y = -\frac{b}{2}$ to $y = \frac{b}{2}$.

The hydrodynamic moment acting on the dam, normalized with respect to $\rho_0 a h^3$, is obtained by integrating (2.29) multiplied by z with respect to z from z = 0 to z = h. This yields

$$C_{mi} \cos \omega t + C_{mo} \sin \omega t = C_m \cos (\omega t - \theta_m), \tag{2.31a}$$

where

$$C_m = (C_{mi}{}^2 + C_{mo}{}^2)^{1/2}, \ \theta_m = \tan^{-1} (C_{mo}/C_{mi}), \tag{2.31b}$$

$$C_{mi} = C_{mi}{}^{0} + \sum_{j=1}^{J} \frac{\ddot{Y}_j^*(\omega)}{a} C_{mi}{}^{j}, \tag{2.31c}$$

$$C_{mo} = C_{mo}{}^{o} + \sum_{j=1}^{J} \frac{\ddot{Y}_j^*(\omega)}{a} C_{mo}{}^{j}, \qquad (2.31d)$$

$$C_{mi}{}^{j} = - \frac{1}{h} \operatorname{Re} \{ \frac{G_o}{(k_o h)^2} \psi_{jo}(0,y) + \sum_{m=1}^{\infty} \frac{G_m}{(k_m h)^2} \psi_{jm}(0,y) \} , \qquad (2.31e)$$

$$C_{mo}^{j} = - \frac{1}{h} \operatorname{Im} \{ \frac{G_o}{(k_o h)^2} \psi_{jo}(0,y) + \sum_{m=1}^{\infty} \frac{G_m}{(k_m h)^2} \psi_{jm}(0,y) \} \quad (j = 0,1,2,\ldots J), \qquad (2.31f)$$

and

$$G_o = k_o h \; Q_o \; (1-C) + 1, \qquad (2.31g)$$

$$G_m = k_m h \; Q_m \; (1-C) - 1. \qquad (2.31h)$$

The total moment coefficient can be obtained by integrating (2.31) with respect to y from $y = - \frac{b}{2}$ to $y = \frac{b}{2}$.

2.5. Complex Frequency Response

It is to be noted that the hydrodynamic pressure $P(x,y,z,t)$ on the dam has been expressed in terms of the unknown complex frequency response for the generalized acceleration $\ddot{Y}_j^*(\omega)$, which is determined as follows.

Equation (2.1) corresponding to the jth-mode vibration of the dam, due to a ground acceleration $ae^{-i\omega t}$ at the base, can be written as

$$[M_j + \frac{F_{2j}(\omega)}{a}]\ \ddot{Y}_j(t) + 2\xi_j\omega_j M_j\dot{Y}_j(t) + \omega_j^2 M_j Y_j(t)$$

$$= - [\Delta a E_j + F_{oj}(\omega)]e^{-i\omega t}, \qquad (2.32)$$

where

$$M_j = \int_0^H \int_{-\frac{b}{2}}^{\frac{b}{2}} m(y,z)\ f_j^{\,2}\ (y,z)\ dy\ dz, \qquad (2.33a)$$

$$E_j = \int_0^H \int_{-\frac{b}{2}}^{\frac{b}{2}} m(y,z)\ f_j(y,z)\ dy\ dz, \qquad (2.33b)$$

$$F_{oj}(\omega) = \int_0^h \int_{-\frac{b}{2}}^{\frac{b}{2}} P_o^*(y,z;\omega)\ f_j(y,z)\ dy\ dz, \qquad (2.33c)$$

$$F_{2j}(\omega) = \int_0^h \int_{-\frac{b}{2}}^{\frac{b}{2}} P_j^*(y,z;\omega)\ f_j(y,z)\ dy\ dz, \qquad (2.33d)$$

in which $m(y,z)$ is the mass distribution for the dam, ξ_j is the damping ratio, ω_j is the natural frequency corresponding to the jth-mode of the dam, $P_j^*(y,z;\omega)$ is the complex frequency response of $P_j(0,y,z,t)$, and Δ is defined in (2.3).

Substituting (2.4) into (2.32), the complex frequency response for a generalized acceleration is obtained as

$$\ddot{Y}_j^*(\omega) = \frac{\Delta a E_j + F_{oj}(\omega)}{M_j[(\frac{\omega_j}{\omega}) - 2i\,\xi_j(\frac{\omega_j}{\omega}) - 1] - \frac{F_{2j}(\omega)}{a}} . \qquad (2.34)$$

The generalized coordinates are obtained by integrating $\ddot{Y}_j(t) = \ddot{Y}_j^*(\omega)\, e^{-i\omega t}$ twice with respect to time:

$$Y_j(t) = -\frac{1}{\omega^2}\, \ddot{Y}_j^*\,(\omega)\, e^{-i\omega t} . \qquad (2.35)$$

Thus, the displacement of the dam can be determined from (2.2) and (2.35).

Since the displacement of the dam relative to the base is expressed as a linear combination of the first J normal-mode shapes of the dam itself, the hydrodynamic pressure on the dam can be determined from (2.29) and (2.34).

CHAPTER III

NUMERICAL METHODS

In Chapter II, the velocity potential is expressed analytically in terms of the function $\psi_{jm}(x,y)$. In order to complete the solution for the velocity potential ϕ, it is necessary to determine the function $\psi_{jm}(x,y)$ which satisfies the Helmholtz equation and the appropriate boundary conditions. The solution of Helmholtz equation can be expressed in integral forms as a function of the values of ψ_{jm} and $\partial\psi_{jm}/\partial n$ on the boundary ∂D.

3.1. Boundary-Integral-Equation Method

By applying Green's identity formula and choosing the Hankel function of the first kind and zeroth order, $H_o^{(1)}(\mu_m r)$ as the fundamental solution of the Helmholtz equation (2.24), the function ψ_{jm} at any position $\vec{x}$ inside the reservoir can be expressed as (see (A.9) in Appendix A.1)

$$\psi_{jm}(\vec{x}) = -\frac{i}{4}\int_{\partial D} [\psi_{jm}(\vec{x}_k)\frac{\partial}{\partial n}(H_o^{(1)}(\mu_m r)) - H_o^{(1)}(\mu_m r)\frac{\partial}{\partial n}\psi_{jm}(\vec{x}_k)]$$

$$ds(\vec{x}_k) \quad (m \le M), \tag{3.1}$$

where $\vec{x}_k$ is the position vector of a boundary point, r is the distance $|\vec{x} - \vec{x}_k|$, and n is in the outward normal direction. The integration is performed along the boundary ∂D of the reservoir travelling in the counter-clockwise direction. If the point $\vec{x}(x,y)$ approaches a boundary point from the interior of the reservoir, then the factor $i/4$ in (3.1) should be replaced by $i/2$ for a smooth boundary or $i\pi/2\alpha$ for a pointed boundary with an interior angle α.

Equation (3.1) leads directly to a solution of $\psi_{jm}(\vec{x})$ anywhere in the reservoir if both ψ_{jm} and $\partial\psi_{jm}/\partial n$ are known everywhere on the boundary. Although $\partial\psi_{jm}/\partial n$ is known from the boundary condition, ψ_{jm} is not known on the boundary. In order to determine the values of ψ_{jm} on the boundary, the field point $\vec{x}$ is allowed to approach a boundary point $\vec{x}_i$. If the boundary is sectionally smooth, (3.1) reduces to (see A.10))

$$\psi_{jm}(\vec{x}_i) = -\frac{i}{2}\int_{\partial D} [\psi_{jm}(\vec{x}_k)\frac{\partial}{\partial n}(H_0^{(1)}(\mu_m r)) - H_0^{(1)}(\mu_m r)\frac{\partial}{\partial n}\psi_{jm}(\vec{x}_k)]\, ds(\vec{x}_k). \tag{3.2}$$

Therefore the values of ψ_{jm} on the boundary can be obtained by solving (3.2). Consequently, the function $\psi_{jm}(\vec{x})$ can be determined anywhere inside the reservoir from (3.1).

Solutions of (2.25) can be obtained by the same method. Let $K_0(\beta_m r)$ be the modified Bessel function of the second kind and zeroth order. The function ψ_{jm} at any point $\vec{x}$ inside the reservoir can be expressed as (see (A.15))

$$\psi_{jm}(\vec{x}) = -\frac{1}{2\pi}\int_{\partial D}\left[\psi_{jm}(\vec{x}_k)\frac{\partial}{\partial n}K_o(\beta_m r) - K_o(\beta_m r)\frac{\partial}{\partial n}\psi_{jm}(\vec{x}_k)\right]$$

$$ds(\vec{x}_k) \quad (m > M), \tag{3.3}$$

where the notation is defined as before. If the point $\vec{x}$ approaches a boundary point from the interior of the reservoir, then the factor $1/2\pi$ in (3.3) should be replaced by $1/\pi$ for a smooth boundary or $1/\alpha$ for a pointed boundary with an interior angle α.

Allowing the field point $\vec{x}$ to approach a smooth boundary point $\vec{x}_i$, we have

$$\psi_{jm}(\vec{x}_i) = -\frac{1}{\pi}\int_{\partial D}\left[\psi_{jm}(\vec{x}_k)\frac{\partial}{\partial n}K_o(\beta_m r) - K_o(\beta_m r)\frac{\partial}{\partial n}\psi_{jm}(\vec{x}_k)\right]$$

$$ds(\vec{x}_k). \tag{3.4}$$

Therefore, by (3.3) and (3.4), (2.25) can be solved everywhere inside the reservoir.

3.2. Matrix Representation of the Solution

In order to solve (3.2) for values of ψ_{jm} on the boundary for an arbitrarily shaped reservoir, the integral equation will be approximated by a matrix equation. The entire boundary of the reservoir is divided into a sufficiently large number of segments, N, where along each segment the average values of

$$\psi_{jm}(\vec{x}_k),\ \frac{\partial\psi_{jm}}{\partial n}(\vec{x}_k),\ H_o^{(1)}(\mu_m r),\ \frac{\partial}{\partial n} H_o^{(1)}(\mu_m r)$$

on that segment are used. Then the integral in (3.2) can be replaced by a finite summation,

$$\psi_{jm}(\vec{x}_i) = -\frac{i}{2}\sum_{k=1}^{N}[\psi_{jm}(\vec{x}_k)\frac{\partial}{\partial n}H_o^{(1)}(\mu_m r_{ik}) - H_o^{(1)}(\mu_m r_{ik})\frac{\partial}{\partial n}\psi_{jm}(\vec{x}_k)]\Delta s_k, \tag{3.5}$$

where

r_{ik} is the distance between the points $\vec{x}_i$ and $\vec{x}_k$ and is defined as $r_{ik} = |\vec{x}_i - \vec{x}_k| = r_{ki}$,

$\vec{x}_i$ is the position vector for the field point on the boundary,

$\vec{x}_k$ is the position vector for the source point on the boundary, and

Δs_k is the length of the kth segment of the boundary.

The segments of the boundary are numbered counter-clockwise. It should be noted that because of this approximate presentation of the boundary, the original curved boundary is replaced by a boundary composed of straight-line segments.

Equation (3.5) can be written in a matrix form as

$$(\frac{i}{2} G_n + I)\ \underline{X} = \frac{i}{2}\ G\underline{Y} \qquad (m \le M), \tag{3.6}$$

where

$$\underline{X} = \psi_{jm}(\vec{x}_k) \qquad k = 1,2,...N, \tag{3.7a}$$

$$\underline{Y} = \frac{\partial \psi_{jm}}{\partial n}(\vec{x}_k) \qquad k = 1,2,...N, \tag{3.7b}$$

$$I_{ik} = \delta_{ik} \begin{cases} 1 \text{ if } i = k \\ 0 \text{ if } i \neq k \end{cases} \qquad \begin{matrix} i = 1,2,...N, \\ k = 1,2,...N, \end{matrix} \tag{3.7c}$$

$$(G_n)_{ik} = \frac{\partial}{\partial n}(H_0^{(1)}(\mu_m r_{ik}))\,\Delta s_k \qquad k = 1,2,...N, \tag{3.7d}$$

$$(G)_{ik} = H_0^{(1)}(\mu_m r_{ik})\,\Delta s_k \qquad k = 1,2,...N. \tag{3.7e}$$

Evaluation of these matrix elements will be discussed in the next section. It should be noted that special care must be taken in evaluating the matrices, especially for the element i=k.

To solve (3.4), the same approximate method is used in which the entire boundary of the reservoir is divided into N segments. Thus, (3.4) can be written in a finite summation form

$$\psi_{jm}(\vec{x}_i) = -\frac{1}{\pi}\sum_{k=1}^{N}[\psi_{jm}(\vec{x}_k)\frac{\partial}{\partial n}K_o(\beta_m r_{ik}) - K_o(\beta_m r_{ik})\frac{\partial}{\partial n}\psi_{jm}(\vec{x}_k)]\Delta s_k \tag{3.8}$$

or written in a matrix form as

$$(\frac{1}{\pi}U_n + I)\,\underline{Z} = \frac{1}{\pi}U\,\underline{W} \qquad (m > M), \tag{3.9}$$

where

$$\underline{Z} = \psi_{jm}(\vec{x}_k) \qquad k = 1,2,\ldots N, \qquad (3.10a)$$

$$\underline{W} = \frac{\partial \psi_{jm}}{\partial n}(\vec{x}_k) \qquad k = 1,2,\ldots N, \qquad (3.10b)$$

$$I_{ik} = \delta_{ik} \begin{cases} 1 \text{ if } i = k \\ 0 \text{ if } i \neq k \end{cases} \qquad \begin{matrix} i = 1,2,\ldots N, \\ k = 1,2,\ldots N, \end{matrix} \qquad (3.10c)$$

$$(U_n)_{ik} = \frac{\partial}{\partial n}(K_o(\beta_m r_{ik}))\,\Delta s_k \qquad k = 1,2,\ldots N \qquad (3.10d)$$

$$(U)_{ik} = K_o(\beta_m r_{ik})\,\Delta s_k \qquad k = 1,2,\ldots N \qquad (3.10e)$$

3.3. Evaluation of Matrices

In Section 3.2 the formulation of an approximate solution to the integral equation is discussed. In this section the method for evaluating the matrices defined in (3.6) and (3.9) will be discussed.

3.3.1. Matrix Elements Defined in (3.6)

(i) Off-diagonal elements of matrix G_n

As defined in (3.5), the notation $\vec{x}_i(x_i, y_i)$ ($i = 1,2,\ldots N$) refers to the field points, and $\vec{x}_k(x_k, y_k)$ ($k = 1,2,\ldots N$) refers to the source points. The elements $(G_n)_{ik}$ for $i \neq k$ can be evaluated as follows:

$$(G_n)_{ik} = \frac{\partial}{\partial n} (H_0^{(1)} (\mu_m r_{ik})) \Delta s_k$$

$$= - \mu_m [J_1 (\mu_m r_{ik}) + i Y_1 (\mu_m r_{ik})] \frac{\partial r_{ik}}{\partial n} \Delta s_k, \qquad (3.11)$$

where J_1 and Y_1 are Bessel functions of the first and second kind of order 1, and $r_{ik} = \sqrt{(x_i - x_k)^2 + (y_i - y_k)^2}$ is the distance between the mid-points of the ith segment and the kth segment of the boundary.

The term $\frac{\partial r_{ik}}{\partial n}$ in (3.11) can be written as

$$\left(\frac{\partial r_{ik}}{\partial n}\right)_k = \frac{\partial r_{ik}}{\partial x_k} \left(\frac{\partial x}{\partial n}\right)_k + \frac{\partial r_{ik}}{\partial y_k} \left(\frac{\partial y}{\partial n}\right)_k. \qquad (3.12)$$

In (3.12), the differentiation with respect to the outward normal direction on the boundary can be changed into that in the tangential direction along the boundary by the relations

$$\frac{\partial x}{\partial n} = \frac{\partial y}{\partial s}, \; \frac{\partial y}{\partial n} = - \frac{\partial x}{\partial s}. \qquad (3.13)$$

Performing the differentiation of $\frac{\partial r_{ik}}{\partial x_k}$ and $\frac{\partial r_{ik}}{\partial y_k}$ in (3.12) and incorporating the definition of r_{ik} yield

$$\left(\frac{\partial r_{ik}}{\partial n}\right)_k = - \frac{x_i - x_k}{r_{ik}} \left(\frac{\partial y}{\partial s}\right)_k + \frac{y_i - y_k}{r_{ik}} \left(\frac{\partial x}{\partial s}\right)_k. \qquad (3.14)$$

Writing (3.14) in a difference form, we have

$$\left(\frac{\partial r_{ik}}{\partial n}\right)_k \approx - \frac{x_i - x_k}{r_{ik}} \left(\frac{\Delta y}{\Delta s}\right)_k + \frac{y_i - y_k}{r_{ik}} \left(\frac{\Delta x}{\Delta s}\right)_k . \qquad (3.15)$$

Therefore, the off-diagonal elements of the matrix G_n can be evaluated by substituting (3.15) into (3.11).

(ii) Diagonal elements of matrix G_n

Since the source and field points are located at the mid-point of straight-line segments which have been used to approximate the boundary, a diagonal element of matrix G_n corresponds to the condition of coincidence of a particular field point and source point. Due to the singular behavior of the Hankel function $H_1^{(1)}(\mu_m r)$ as $\mu_m r \to 0$, special attention must be given in evaluating these diagonal elements.

The asymptotic behavior of $H_1^{(1)}(\mu_m r)$ as $u_m r \to 0$ is

$$\lim_{\mu_m r \to 0} H_1^{(1)}(\mu_m r) \sim \frac{\mu_m r}{2} - i \frac{2}{\pi} \frac{1}{\mu_m r} . \qquad (3.16)$$

Therefore, the diagonal elements of matrix G_n can be evaluated as the limiting value as r approaches zero,

$$(G_n)_{ii} = \lim_{r \to 0} \left(- \mu_m H_1^{(1)} (\mu_m r) \frac{\partial r}{\partial n}\right) \Delta s_i$$

$$= i \frac{2}{\pi} \Delta s_i \lim_{r \to 0} \frac{\frac{\partial r}{\partial n}}{r}. \tag{3.17}$$

The definition of r is

$$r = \sqrt{(x-x_i)^2 + (y-y_i)^2},$$

where (x_i, y_i) are the coordinates of the mid-point of the ith segment on the boundary. Thus the term $\frac{\partial r}{\partial n}$ can be expressed as

$$\frac{\partial r}{\partial n} = \frac{\partial r}{\partial x}\frac{\partial x}{\partial n} + \frac{\partial r}{\partial y}\frac{\partial y}{\partial n}$$

$$= \frac{x-x_i}{r}\left(\frac{\partial y}{\partial s}\right) + \frac{y-y_i}{r}\left(-\frac{\partial x}{\partial s}\right). \tag{3.18}$$

The terms $(x-x_i)$, $(y-y_i)$, $\frac{\partial x}{\partial s}$, and $\frac{\partial y}{\partial s}$ can be expressed in Taylor series in the neighborhood of (x_i,y_i),

$$x-x_i = (x_s)_i \Delta s + (x_{ss})_i \frac{(\Delta s)^2}{2!} + (x_{sss})_i \frac{(\Delta s)^3}{3!} + \dots, \tag{3.19a}$$

$$\frac{\partial x}{\partial s} = (x_s)_i + (x_{ss})_i \Delta s + (x_{sss})_i \frac{(\Delta s)^2}{2!} + \dots, \tag{3.19b}$$

$$\Delta s = |x-x_i|, \tag{3.20}$$

where the subscript s refers to the differentiation with respect to s, the index i means that the values of interest are evaluated at the mid-point of the ith segment. The expressions for $y - y_i$ and $\frac{\partial y}{\partial s}$ can be obtained in exactly the same way.

Thus the term $\lim\limits_{r \to 0} \frac{\partial r}{\partial n}/r$ in (3.17) can be evaluated by using the definition of r, (3.19) and (3.20). Neglecting the higher-order terms in these relations reduces them to

$$\lim_{r \to 0} \frac{\frac{\partial r}{\partial n}}{r} = \lim_{\Delta s \to 0} \frac{\frac{\partial r}{\partial n}}{r} \approx \frac{(x_s y_{ss} - x_{ss} y_s)_i}{2}. \tag{3.21}$$

Therefore, the diagonal elements of the matrix G_n can be found from (3.17) as

$$(G_n)_{ii} = \frac{i}{\pi} (x_s y_{ss} - x_{ss} y_s)_i \, \Delta s_i. \tag{3.22}$$

In (3.22), the first and second derivatives are evaluated at the mid-point of the ith segment of the boundary.

For a boundary which is originally composed of straight lines, the value of $x_s y_{ss}$ and $y_{ss} x_s$ in (3.22) are both equal to zero. Hence, the diagonal elements of matrix G_n are equal to zero. For a curved boundary which has been approximated by straight-line segments, the expression of the first and second derivatives, x_s and x_{ss}, can be written in a difference form as

$$x_s = \frac{x_{i+\frac{1}{2}} - x_{i-\frac{1}{2}}}{\Delta s_i}, \tag{3.23a}$$

$$x_{ss} = \frac{8}{\Delta s_{i-1} + 2\Delta s_i + \Delta s_{i+1}} \left[\frac{x_{i+1} - x_i}{\Delta s_{i+1} + \Delta s_i} - \frac{x_i - x_{i-1}}{\Delta s_{i-1} + \Delta s_i}\right], \tag{3.23b}$$

where x_i is the x coordinate at the mid-point of the ith segment of the boundary, $x_{i-\frac{1}{2}}$ is the x coordinate at the beginning of the ith segment and $x_{i+\frac{1}{2}}$ is the x coordinate at the end of the ith segment of the boundary; Δs_{i-1}, Δs_i, and Δs_{i+1} are the lengths of the (i-1)th, ith, and (i+1)th segments of the boundary. The derivatives y_s and y_{ss} can be evaluated in a similar way by changing x to y in (3.23).

(iii) Off-diagonal elements of matrix G

The elements $(G)_{ik}$ for $i \neq k$ can be evaluated directly from the expression:

$$(G)_{ik} = H_0^{(1)} (\mu_m r_{ik}) \Delta s_k = [J_0(\mu_m r_{ik}) + iY_0(\mu_m r_{ik})] \Delta s_k. \qquad (3.24)$$

(iv) Diagonal elements of matrix G

The diagonal elements of matrix G correspond to the case of i=k in (3.24). As before, due to the singular behavior of the function $H_0^{(1)}(\mu_m r)$, special attention must be given in evaluating the diagonal elements of matrix G. Using the asymptotic formula of $H_0^{(1)}(\mu_m r)$ as the argument $\mu_m r$ approaches zero,

$$\lim_{\mu_m r \to 0} H_0^{(1)} (\mu_m r) \approx 1 + i \frac{2}{\pi} (\ln \frac{\mu_m r}{2} + \gamma), \qquad (3.25)$$

we have the average value of $(G)_{ii}$ as

$$(G)_{ii} = \{\frac{1}{\frac{1}{2}\Delta s_i} \int_0^{\frac{1}{2}\Delta s_i} [1+i\,\frac{2}{\pi}\,(\ln \frac{\mu_m r}{2} + \gamma)]\, dr\}\ \Delta s_i$$

$$= \{1 + i\,\frac{2}{\pi}\,(\ln \frac{\mu_m \Delta s_i}{4} - 1 + \gamma)\}\ \Delta s_i, \qquad (3.26)$$

where $i = 1,2,...N$, and $\gamma = 0.577216$ is Euler's constant.

3.3.2. Matrix Elements Defined in (3.9)

The elements of the matrices defined in (3.9) can be evaluated by the same method as described in Section (3.3.1).

(i) Off-diagonal elements of U_n

$$(U_n)_{ik} = \beta_m K_1\ (\beta_m r_{ik})\ [\frac{x_i - x_k}{r_{ik}}\ (\frac{\Delta y}{\Delta s})_k - \frac{y_i - y_k}{r_{ik}}\ (\frac{\Delta x}{\Delta s})_k]\ \Delta s_k \qquad (3.27)$$

where $K_1\ (\beta_m r)$ is modified Bessel function of the second kind and first order.

(ii) Diagonal elements of U_n

Special care is given to evaluate the diagonal elements of U_n. By using the asymptotic behavior of $K_1\ (\beta_m r)$ as $\beta_m r \to 0$,

$$\lim_{\beta_m r \to 0} K_1(\beta_m r) \approx \frac{1}{\beta_m r}, \tag{3.28}$$

the diagonal elements of U_n can be evaluated as

$$(U_n)_{ii} = \frac{1}{2}\,(y_s x_{ss} - x_s y_{ss})_i\, \Delta s_i, \tag{3.29}$$

where x_s, y_s, x_{ss} and y_{ss} are given by (3.23).

(iii) Off-diagonal elements of U

$$(U)_{ik} = K_o(\beta_m r_{ik})\, \Delta s_k. \tag{3.30}$$

(iv) Diagonal elements of U

Using the asymptotic formula of $K_o\,(\beta_m r)$ as $\beta_m r \to 0$,

$$\lim_{\beta_m r \to 0} K_o(\beta_m r) \approx -\left(\ell n\, \frac{\beta_m r}{2} + \gamma\right), \tag{3.31}$$

and performing the integration to determine the average value of this function over the length of the segment interested, we obtain

$$(U)_{ii} = -\left[\ell n\, \frac{\beta_m \Delta s_i}{4} - 1 + \gamma\right] \Delta s_i \tag{3.32}$$

where γ is Euler's constant.

After the matrices are evaluated, the only terms left to be determined to solve the matrix equation are the elements which involve the normal derivatives on the boundary. However, the normal derivatives are given by the boundary conditions. Dividing the boundary into N segments and assuming no attenuation of ground excitations between the dam and the far end of the reservoir, we can replace A(x,y) at the ith segment by $(\frac{\Delta y}{\Delta s})_i$ for longitudinal excitations or $(-\frac{\Delta x}{\Delta s})_i$ for lateral excitations. For a flexible dam, the integral $\int_0^h f_j(y,z) \cos (k_m z)\, dz$ can be evaluated by employing the trapezoidal rule. It should be noted that $\frac{\partial}{\partial n} = -\frac{\partial}{\partial x}$ at $x = 0$.

CHAPTER IV

RESULTS AND DISCUSSION

A theory for an arbitrarily shaped reservoir has been presented in Chapters II and III. The numerical method will be tested by checking the results with existing analytical solutions for a system which consists of a rigid dam and reservoir with a simple geometric shape. A rectangular-plate dam will be used to investigate the flexibility effect on the response of a three-dimensional dam-reservoir system.

4.1. Response of a Rigid Dam

A rectangle, a circle, and a semi-circle are chosen as the representative plan-form shapes of a simple reservoir (see Fig. 2) to test the present numerical method. These three shapes are chosen for several reasons: (1) existence of the corresponding theoretical, closed-form solutions; (2) the boundary of a rectangle represents an extreme case that it is composed of four straight lines, along each of which the direction of the tangent to the boundary remains constant; (3) the boundary of a circle is another extreme case for which the tangent to the boundary changes its direction continuously;

and (4) the boundary of a semi-circle contains one straight line and a circular arc.

The dimensionless pressure, force, and moment coefficients are given by (2.29), (2.30) and (2.31) respectively. The terms with $j = 0$ are the only terms for the response of a rigid dam. The local pressure coefficient is dependent on the dimensionless groups z/h, y/h, C (defined in (2.22)), B (defined in (2.23c)), and the size of the reservoir. The force and moment coefficients are, however, independent of z/h, but depend on all other parameters. B is a measure of the compressibility of water. $B = 0$ means the water is treated as incompressible. C is a ratio of the gravity effect to the inertial effect due to harmonic ground motion; $C = 0$ indicates no surface waves.

The period of the ground acceleration, T, during a typical earthquake may range from 0.1 to 10 seconds. If the reservoir height h, is assumed to be 300 ft, then the maximum value of B is approximately 4 and that of C is 0.27. Since C is inversely proportional to h and B is directly proportional to h, the value of B increases as C decreases.

4.1.1. Rectangular Reservoir

A theoretical solution for the earthquake response of a three-dimensional rectangular dam-reservoir system has been obtained by Huang and Chwang (1982). The hydrodynamic pressure is not a function of y/h for a longitudinal excitation. By dividing the boundary into N segments, the numerical results will be obtained and compared with the theoretical ones.

It is expected that as the number of segments, into which the boundary of the reservoir is divided, is increased, the numerical results will agree better with the theoretical solutions. A comparison of the theoretical and numerical results for three different values of N with C = 0 and C = 0.2 are shown in Figs. 3 and 4 respectively. For the case with C = 0 (no surface waves), it is seen that as N increases, the numerical results of the approximate method agree better with the theoretical predictions. However, with C = 0.2, there is a large difference between the theoretical and numerical results near free surface (z/h = 1) for N = 40, and the effect of N is significant. With the presence of surface waves, a sufficiently large N should be taken that the maximum segment length is much less than the wave length. Based on the numerical results, Lee (1969) suggested that the ratio of the length of the largest segment to the smallest wave length should be less than 0.1. N = 78 is used in the following study for a rectangular reservoir.

The influence of the reservoir length, ℓ/h, on the pressure, force and moment coefficients are shown in Figs. 5 and 6. These coefficients increase monotonically as ℓ/h increases, and remain almost constant when ℓ/h is greater than 5. The limiting value of C_p at z/h = 0, and C_f and C_m as $\ell/h \to \infty$ are 0.742, 0.543 and 0.218 respectively (Huang and Chwang (1982)).

The effect of C on the hydrodynamic pressure is shown in Fig. 7. It should be noted that the pressure at the undisturbed water surface ($z/h = 1$) is no longer zero when surface waves are present. In fact, the surface wave can play an important role as seen in Fig. 7 for $C = 0.15$ and $C = 0.25$. The pressure at the bottom of the dam decreases as C increases, but it is oscillatory near water surface.

The effect of B on the hydrodynamic pressure for $C = 0$ is shown in Fig. 8. It is found that when $B = k_1h$, first resonance occurs. Resonance also occurs at frequencies $\omega = c_o k_m$ ($m = 2,3,...$). Therefore, when B is greater than k_nh (n fixed), there are n modes of standing waves (see (2.18) and (2.24b)). As a result, the hydrodynamic pressure becomes oscillatory. This can clearly be seen in Fig. 9, which shows the corresponding force coefficient for $C = 0$ and $C = 0.05$. We note that the force coefficient with $C = 0.05$ is less than that with $C = 0$ when B is small, and the resonance frequencies are slightly higher when the wave is present.

All the results presented so far are due to a longitudinal excitation. For a lateral excitation, the results are shown in Fig. 10 and Fig. 11.

The hydrodynamic pressure coefficient C_p at various values of y/h is shown in Fig. 10. We note that the magnitude of C_p increases as y/h increases and C_p is zero at the plane $y = 0$ (i.e. center of dam). The value of C_p due to the compressibility effect is also found to be oscillatory for large values of B, as shown in Fig. 11.

4.1.2. Circular Reservoir

Theoretical analysis for the response of a circular dam-reservoir system was made by Kadle and Chwang (1982). The local pressure coefficient C_p depends on the dimensionless parameters R/h, z/h, C and B, where R is the radius of the circular reservoir. The force and moment coefficients, however, are independent of z/h, but depend on all other parameters. Only excitations in the x direction are considered in circular and semi-circular reservoirs.

The pressure distribution at the dam face is shown in Fig. 12 for an incompressible fluid without surface waves (B = 0, C = 0), for N = 72 and varying values of R/h. The pressure at any height increases with increasing R/h, until it reaches a maximum for a certain value of R/h. Then, with further increase in R/h, the pressure diminishes and attains a finite value as $R/h \to \infty$. Similar behavior is also found for the force and moment coefficients, C_f and C_m, as seen in Fig. 13. The theoretical values of C_p at z/h = 0, C_f and C_m as $R/h \to \infty$ are 0.742, 0.543 and 0.218 respectively, which are precisely the values obtained for a rectangular reservoir as $\ell/h \to \infty$.

The behavior of the pressure distribution with an increase in R/h can be explained. Initially, the pressure increases as the amount of the fluid in the reservoir increases, as long as the total mass in the reservoir is less than the "added mass". It keeps increasing until the total mass exceeds the "added mass". There is another factor affecting the pressure at the dam face. This is the curvature of the side walls near the dam. When the reservoir is small, there is a component of the hydrodynamic pressure at the dam face, due to the side walls. However, when the reservoir is large enough, this effect is negligible. Hence, the pressure falls and stabilizes as $R/h \to \infty$.

The variation of the pressure coefficient C_p with the compressibility parameter B is shown in Fig. 14 for $R/h = 5$ and $C = 0$. The pressure increases with small B. However, it becomes oscillatory when B is large. The force coefficient C_f versus the compressibility parameter B is shown in Fig. 15 with $C = 0$ and $C = 0.05$. Again, resonance occurs when $B > \frac{\pi}{2}$. With a small wave-effect parameter C, the force coefficient is decreased and the resonance frequencies are slightly higher.

The hydrodynamic pressure distribution on a dam for various wave-effect parameter C is shown in Fig. 16. The curves are similar to the ones for a rectangular reservoir. C_p is oscillatory near the water surface.

4.1.3. Semi-Circular Reservoir

Theoretical results for the response of a semi-circular dam-reservoir was obtained by Kadle and Chwang (1982). The pressure coefficient depends on the dimensionless parameters R/h, r/R, C and B. The force and moment coefficients, however, are independent of z/h but depend on all other parameters.

The pressure coefficient C_p at the dam face is shown in Fig. 17 for a reservoir of size R/h = 5, for N = 68 and various r/R. The fluid is considered to be incompressible with no surface waves (B = 0, C = 0). The maximum value for any fixed location r/R is attained at the bottom of the dam (z/h=0). Also, the maximum C_p at any height occurs at the central plane of the dam (r/R = 0), and decreases slightly as r/R increases to 1.

The overall behavior of a semi-circular reservoir is similar to that of a rectangular reservoir. The influence of R/h on the force and moment coefficients are shown in Fig. 18. The hydrodynamic pressure distribution at the center of a dam for various values of the wave-effect parameter C is shown in Fig. 19. The compressibility effect on the force coefficient C_f is shown in Fig. 20 for C = 0 and C = 0.05.

4.2. Response of a Flexible-Plate Dam

A rectangular plate dam in a rectangular reservoir or in a semi-circular reservoir is used to illustrate the flexibility effect on the seismic response of dams. Rectangular plates with width to height ratios of 2 and 10 are chosen as examples. The plate is fixed (clamped) at the bottom (z = 0) and at two vertical side boundaries ($y = \pm \frac{b}{2}$), and is free at the top (z = H). For simplicity, the plate height is assumed to be equal to the reservoir depth (H = h) in the following study.

The natural frequencies ω_j and normal-mode shapes $f_j(y,z)$ ($j = 1,2,3,...$) for a rectangular plate with width b, height h and thickness d, can be obtained by solving the classical equation for a free vibrational plate (Gorman, 1982)

$$\frac{\partial^4 f_j}{\partial y^4} + 2\frac{\partial^4 f_j}{\partial y^2 \partial z^2} + \frac{\partial^4 f_j}{\partial z^4} - \frac{m\omega_j^2}{D} f_j = 0, \tag{4.1a}$$

where

$$D = \frac{E\, d^3}{12(1-\nu^2)} \tag{4.1b}$$

is the flexural rigidity of the plate, m is mass of the plate per unit area, E is Young's modulus and ν is the Poisson ratio for the plate material.

At fixed (clamped) boundaries, the boundary conditions for $f_j(y,z)$ are

$$f_j\ (\pm\, b/2,z) = \frac{\partial f_j(\pm b/2,z)}{\partial y} = 0, \tag{4.2a}$$

$$f_j\ (y,0) = \frac{\partial f_j(y,0)}{\partial z} = 0. \tag{4.2b}$$

At the free boundary $z = h$, we require

$$\frac{\partial^2 f_j}{\partial z^2} + \nu\frac{\partial^2 f_j}{\partial y^2} = 0 \qquad \text{at } z = h, \tag{4.2c}$$

$$\frac{\partial^3 f_j}{\partial z^3} + (2-\nu)\frac{\partial^3 f_j}{\partial y^2 \partial z} = 0 \qquad \text{at } z = h. \tag{4.2d}$$

The solution of equation (4.1) satisfying the boundary conditions (4.2) was obtained by Gorman (1982, pp. 204-219) in terms of six sets of infinite Fourier series, three for symmetric modes and three for antisymmetric modes. The dimensionless eigenvalues λ_j^2 defined by

$$\lambda_j^2 = \omega_j b^2 (m/D)^{1/2} \tag{4.3}$$

are functions of the Poisson ratio ν and the aspect ratio b/h. Therefore, the jth eigenvalue λ_j^2 can be determined numerically by substituting the six sets of truncated Fourier series into equation (4.1), then applying the boundary conditions (4.2), and finally equating the determinant of the finite-dimensional characteristic matrix to zero.

The first four mode shapes and the corresponding dimensionless frequencies λ_j^2 for a rectangular plate with ν = 0.17 and aspect ratio of 2 and 10 are shown in Fig. 21. We note that, for a plate with an aspect ratio of 2, the first, third, and fourth mode are symmetric with respect to the center of the plate and the second mode is antisymmetric. For a plate with an aspect ratio of 10, the first and the third modes are symmetric and the second and the fourth modes are antisymmetric.

The complex frequency response for a generalized acceleration $\ddot{Y}_j^*(\omega)$ for jth-mode is determined from (2.34). In addition to the dimensionless parameters of the fluids, $\ddot{Y}_j^*(\omega)$ also depends on the ratio of the natural frequency of the dam to the exciting frequency, ω_j/ω, the rigidity of the dam, and the mass ratio of water to the dam, S, where S is defined as $\frac{\rho_0 h}{m}$ (Mei, 1979). The following parameters are used in this study:

$$b/h = 2 \text{ and } 10, \quad H/h = 1, \quad d/h = 0.3,$$

$$c_0 = 4720 \text{ ft/sec},$$

$$E = 7.2 \times 10^8 \text{ lb/ft}^2,$$

$$\nu = 0.17,$$

$$S = 1.34.$$

The material constants E, ν and S correspond to the concrete. An artificial damping ratio of 0.05 for concrete is introduced.

A rectangular reservoir with b/h = 2 and ℓ/h = 10, and a semi-circular reservoir with R/h = 5, which corresponds to a dam with b/h = 10, are considered here as representative shapes of a reservoir.

The pressure distribution on one half of a dam for each mode are shown in Fig. 22. We note that the pressure distribution at the center of the dam is zero for antisymmetric modes. Figure 23 shows a comparison between the pressure distributions on a dam when different numbers of modes are considered. It is seen that only the first mode has a significant effect. In the following study, 4 modes are used.

The hydrodynamic force response is shown in Figs. 24 and 25 for a rectangular reservoir (b/h = 2) and a semi-circular reservoir (b/h = 10), respectively.

The first four natural frequencies normalized by c_0/h are 1.83, 4.08, 5.94, and 7.44 for a dam with b/h = 2, and are 0.83, 0.91, 1.04 and 1.21 for a dam with b/h = 10. They are shown on the abscissas in Fig. 24 and Fig. 25 by open circles.

Resonance occurs at the natural frequencies of the coupled system. The natural frequency of the dam plays an important role in the hydrodynamic response. In the case of b/h = 10 (Fig. 25), the natural frequencies of the dam alone are less than the resonance frequencies of the coupled system for a semi-circular reservoir. The hydrodynamic force is reduced when the exciting frequency is smaller than the natural frequency of the dam alone. However, it increases considerably when the exciting frequency gets larger. The first two natural frequencies for the coupled system are smaller than the first resonance frequency of a rigid dam-reservoir system. In the case of b/h = 2 (Fig. 24), the first natural frequency of the dam alone is greater than the first one of the rigid dam-reservoir system. On the other hand, the first fundamental frequency of the coupled system is very close to that of the reservoir. The second natural frequency of the coupled system is between the first two frequencies of the reservoir and is less than that of the dam alone.

The flexibility effect on the response of a coupled system depends on the natural frequencies of the dam and of the reservoir.

It becomes important when the exciting frequency is larger than the natural frequency of the dam alone.

It should be noted that the pressure $P_j^*(x,y;\omega)$ $(j = 1,2,\ldots 4)$ and the complex frequency response of general acceleration $\ddot{Y}_j^*(\omega)$ are coupled. By assuming the exciting amplitude to be small, matrix elements for rigid dam case is adopted to solve the pressure $P_j^*(x,y;\omega)$.

CHAPTER V

CONCLUSIONS AND RECOMMENDATIONS

The hydrodynamic effect of an earthquake on a three-dimensional, arbitrarily shaped dam-reservoir system was analyzed and described. For a ground motion $ae^{-i\omega t}$, a hybrid analytical-numerical method was developed and found to accurately predict the hydrodynamic response. The effect of surface waves and compressibility of the fluid in the reservoir was discussed in detail, with the effect of flexibility of the dam also included. The present results are in good agreement with the analytical solutions derived by Huang and Chwang (1982) and Kadle and Chwang (1982) for rigid dams and reservoirs with simple geometric shapes, such as a rectangle, a circle, or a semi-circle.

In the presence of surface waves, a large segment number N into which the entire boundary is divided should be taken, such that the largest segment length is much less than the smallest wave length. A ratio of one-tenth was suggested. With the presence of surface waves, the pressure is oscillatory and plays an important role near the free surface.

The resonance of the fluid in the reservoir occurs when the compressibility effect parameter B is greater than $\pi/2$ (h/T > 1180 ft/sec). The present method predicts the resonance accurately for an arbitrarily shaped reservoir. The pressure distribution on a dam is affected by the shape of a reservoir. Therefore, three-dimensional dam-reservoir analysis is necessary to calculate the hydrodynamic response (pressure, force and moment).

The flexibility effect is also included in this study. Only the first few normal-modes are important. The flexibility of a dam changes significantly the hydrodynamic pressure force acting on the dam.

For any horizontal excitation, the hydrodynamimc response can be obtained by decomposing it into a longitudinal and a lateral component. The responses obtained here are due to a harmonic ground acceleration. For any arbitrary ground motion, the response can be obtained by integration in the frequency domain.

A linear motion was assumed in this study. In a large variety of practical systems, this assumption may not be valid and the non-linearity effect should be studied.

APPENDIX A

SOLUTION OF THE HELMHOLTZ EQUATION

The derivation of a solution to the two dimensional Helmholtz equation in a bounded domain will be presented in this appendix. For convenience, the subscripts jm and m will be dropped.

A.1. Derivation of Equation (3.1)

Let ∂D be a closed curve bounding a domain D in the x-y plane. Green's second identity gives

$$\int_{\partial D} \left(\psi \frac{\partial \phi}{\partial n} - \phi \frac{\partial \psi}{\partial n}\right) ds = \iint_{D} (\psi \nabla^2 \phi - \phi \nabla^2 \psi)\, dA, \tag{A.1}$$

where $\partial/\partial n$ denotes differentiation along the outward normal direction on the boundary ∂D, ϕ and ψ are regular, twice continuously differentiable functions within the domain D and on the boundary ∂D. Let ψ be a regular solution of the Helmholtz equation

$$\nabla^2 \psi + \mu^2 \psi = 0, \tag{A.2}$$

and ϕ be the fundamental solution of (A.2), $H_0^{(1)}(\mu,r)$, where $H_0^{(1)}$ is the Hankel function of the first kind and zeroth order, which is singular at the origin. Now, let the singularity be located at an interior point $\vec{x}$. To avoid the singularity, Green's second identity will be applied to the domain D_1, bounded by ∂D and by a circle S_ε of radius ε with its center at $\vec{x}$ (see Fig. A.1). Thus, Green's second identity becomes

$$\int_{\partial D} (\psi \frac{\partial \phi}{\partial n} - \phi \frac{\partial \psi}{\partial n})\, ds + \int_{S_\varepsilon} (\psi \frac{\partial \phi}{\partial n} - \phi \frac{\partial \psi}{\partial n})\, ds = \iint_{D_1} (\psi \nabla^2 \phi - \phi \nabla^2 \psi)\, dA. \tag{A.3}$$

Since the singularity is outside the domain D_1, both ϕ and ψ are regular solutions of the Helmholtz equation (A.2). Therefore, the right-hand side of (A.3) equals to zero. Thus, (A.3) reduces to

$$\int_{\partial D} [\psi \frac{\partial}{\partial n} (H_0^{(1)}(\mu r)) - H_0^{(1)}(\mu r) \frac{\partial \psi}{\partial n}]\, ds = - \int_{S_\varepsilon} [\psi \frac{\partial}{\partial n} (H_0^{(1)} (\mu r)) - H_0^{(1)}(\mu r) \frac{\partial \psi}{\partial n}]\, ds, \tag{A.4}$$

where r is measured from the point $\vec{x}$. Note that on the boundary S_ε, $\partial/\partial n = -\partial/\partial r$, (A.4) can be written as

$$\int_{\partial D} [\psi \frac{\partial}{\partial n} (H_0^{(1)}(\mu r)) - H_0^{(1)}(\mu r) \frac{\partial \psi}{\partial n}] ds = \int_{S_\varepsilon} [\psi \frac{\partial}{\partial r} (H_0^{(1)}(\mu r)) - H_0^{(1)}(\mu r) \frac{\partial \psi}{\partial r}]\, ds. \tag{A.5}$$

We now let ε tend to zero. The right-hand side of (A.5) can be written as

$$\lim_{\varepsilon\to 0} \int_{S_\varepsilon} [\psi \frac{\partial}{\partial r} (H_0^{(1)}(\mu r)) - H_0^{(1)}(\mu r) \frac{\partial \psi}{\partial r}] ds. \tag{A.6}$$

By using the asymptotic behavior of the Hankel function for small argument ($\mu r \to 0$)

$$H_0^{(1)}(\mu r) \sim i \frac{2}{\pi} \ln(\mu r), \tag{A.7a}$$

$$\frac{\partial}{\partial r} (H_0^{(1)}(\mu r)) \sim i \frac{2}{\pi} \frac{1}{r}, \tag{A.7b}$$

the limit of (A.6) can be evaluated. The first and second terms in (A.6) reduce to

$$\lim_{\varepsilon\to 0} \int_{S_\varepsilon} \psi \frac{\partial}{\partial r} (H_0^{(1)}(\mu r)) \, ds = \lim_{\varepsilon\to 0} \int_0^{2\pi} \psi (i \frac{2}{\pi} \frac{1}{\varepsilon}) \, \varepsilon \, d\theta$$

$$= 4i \, \psi(\vec{x}), \tag{A.8a}$$

$$\lim_{\varepsilon\to 0} \int_{S_\varepsilon} H_0^{(1)} (\mu r) \frac{\partial \psi}{\partial r} ds = \lim_{\varepsilon\to 0} \int_0^{2\pi} \frac{\partial \psi}{\partial r} (i \frac{2}{\pi} \ln(\mu\varepsilon)) \, \varepsilon \, d\theta = 0. \tag{A.8b}$$

Substitute (A.8) into (A.5), we obtain

$$\psi(\vec{x}) = - \frac{i}{4} \int_{\partial D} [\psi \frac{\partial}{\partial n} (H_0^{(1)}(\mu r)) - H_0^{(1)}(\mu r) \frac{\partial \psi}{\partial n}] \, ds. \tag{A.9}$$

In order to determine the function ψ on the boundary, we let the field point $\vec{x}$ be on the boundary. The circle S_ε in Fig. A.1 reduces to a semi-circle (see Fig. A.2). In the limit as ε tends to zero, the contribution to the integral in (A.8a) from the semi-circle is only half of that due to a complete circle, i.e., $2i\psi(\vec{x})$. Therefore, we have

$$\psi(\vec{x}_i) = -\frac{i}{2}\int_{\partial D} [\psi(\vec{x}_k)\frac{\partial}{\partial n}(H_0^{(1)}(\mu r)) - H_0^{(1)}(\mu r)\frac{\partial}{\partial n}\psi(\vec{x}_k)]\, ds(\vec{x}_k), \tag{A.10}$$

where $r = |\vec{x}_k - \vec{x}_i|$, and both $\vec{x}_i$ and $\vec{x}_k$ are on the boundary ∂D. Similarly, if the point $\vec{x}_i$ is a corner point on the boundary (see Fig. A.3), (A.9) reduces to

$$\psi(\vec{x}_i) = -\frac{\pi i}{2\alpha}\int_{\partial D} [\psi(\vec{x}_k)\frac{\partial}{\partial n}(H_0^{(1)}(\mu r)) - H_0^{(1)}(\mu r)\frac{\partial}{\partial n}\psi(\vec{x}_k)]\, ds(\vec{x}_k), \tag{A.11}$$

where the interior angle α is defined in Fig. A.3. For a smooth curve, α is equal to π, thus (A.11) is identical to (A.10).

A.2. Derivation of Equation (3.3)

Following the same approach described in the previous section, we let ϕ and ψ be regular, twice continuously differentiable functions within the domain D and on the boundary ∂D, we further assume that ψ be a solution of Helmholtz equation

$$\nabla^2\psi - \beta^2\psi = 0, \tag{A.12}$$

and $\phi = K_o(\beta r)$, where K_o is the modified Bessel function of the second kind and zeroth order. Then, Green's second identity becomes

$$\int_{\partial D} [\psi \frac{\partial}{\partial n} K_o(\beta r) - K_o(\beta r) \frac{\partial \psi}{\partial n}] \, ds = \int_{S_\varepsilon} [\psi \frac{\partial}{\partial r} K_o(\beta r) - K_o(\beta r) \frac{\partial \psi}{\partial r}] \, ds. \tag{A.13}$$

Using the asymptotic behavior of the Bessel function for small argument ($\beta r \to 0$)

$$K_o(\beta r) \sim - \ln(\beta r), \tag{A.14a}$$

$$\frac{\partial}{\partial r} K_o(\beta r) \sim - \frac{1}{r}, \tag{A.14b}$$

and letting the radius ε of the small circle approach zero, we have

$$\psi(\vec{x}) = - \frac{1}{2\pi} \int_{\partial D} [\psi(\vec{x}_k) \frac{\partial}{\partial n} K_o(\beta r) - K_o(\beta r) \frac{\partial}{\partial r} \psi(\vec{x}_k)] \, ds(\vec{x}_k). \tag{A.15}$$

If the field point $\vec{x}$ is a boundary point $\vec{x}_i$, (A.15) reduces to

$$\psi(\vec{x}_i) = - \frac{1}{\pi} \int_{\partial D} [\psi(\vec{x}_k) \frac{\partial}{\partial n} K_o(\beta r) - K_o(\beta r) \frac{\partial}{\partial n} \psi(\vec{x}_k)] \, ds(\vec{x}_k). \tag{A.16}$$

If the point $\vec{x}_i$ is a corner point on the boundary (A.19) becomes

$$\psi(\vec{x}_i) = -\frac{1}{\alpha} \int_{\partial D} [\psi(\vec{x}_k) \frac{\partial}{\partial n} K_0(\beta r) - K_0(\beta r) \frac{\partial}{\partial n} \psi(\vec{x}_k)] ds(\vec{x}_k), \qquad (A.17)$$

where the interior angle α is defined in Fig. A.3. For a smooth curve, α is equal to π.

REFERENCES

Chakrabarti, P. and Chopra, A.K. (1973a), "Hydrodynamics Pressure and Response of Gravity Dams to Vertical Earthquake Component", Int. J. Earthq. Eng. Struct. Dyn. 1, 325-335.

Chakrabarti, P. and Chopra, A.K. (1973b), "Earthquake Analysis of Gravity Dams Including Hydrodynamic Interaction", Int. J. Earthq. Eng. Struc. Dyn. 2, 143-160.

Chakrabarti, P. and Chopra, A.K. (1974), "Hydrodynamic Effects in Earthquake Response of Gravity Dams", J. Struct. Division, ASCE, 100, 1211-1224.

Chopra, A.K. (1967), Hydrodynamic Pressures on Dams During Earthquakes", J. Eng. Mech. Division, ASCE, 93, 205-223.

Chopra, A.K. (1968), "Earthquake Behavior of Reservoir-Dam System", J. Eng. Mech. Division, ASCE, 94, 1475-1500.

Chopra, A.K. (1970), "Earthquake Response of Concrete Gravity Dams", J. Eng. Mech. Division, ASCE, 96, 443-454.

Chwang, A.T. (1978), "Hydrodynamic Pressures on Sloping Dams During Earthquakes. Part 2: Exact Theory", J. Fluid Mech. 87, 343-348.

Chwang, A.T. (1979), "Hydrodynamic Pressure on an Accelerating Dam and Criteria for Cavitation", J. Eng. Math., 13, 143-152.

Chwang, A.T. (1981), "Effect of Stratification of Hydrodynamic Pressures on Dams", J. Eng. Math., 15, 49-63.

Chwang, A.T. and Housner, G.W. (1978), "Hydrodynamic Pressures on Sloping Dams During Earthquakes. Part 1: Momentum Method", J. Fluid Mech., 87, 335-341.

Gorman, D.J. (1982), "Free Vibration Analysis of Rectangular Plates", Elsevier North Holland, Inc., New York, NY.

Huang, T.H. and Chwang, A.T. (1982), "Earthquake Effects on Rectangular Dam-Reservoir System", IIHR Report No. 245, Iowa Institute of Hydraulic Research, The University of Iowa.

Kadle, D.S. and Chwang, A.T. (1982), "Hydrodynamic Effect of Earthquake on Circular Dam-Reservoir Systems", IIHR Report No. 246, Iowa Institute of Hydraulic Research, The University of Iowa.

Kotsubo, S. (1959), "Dynamic Water Pressure on Dams due to Irregular Earthquakes", Mem. Fac. Eng., Kyushu Univ., Japan, 18, 119-129.

Kotsubo, S. (1961), "External Forces on Arch Dam During Earthquakes", Mem. Fac. Eng., Kyushu Univ., Japan, 20, 327-366.

Lee, J.J. (1969), "Wave-Induced Oscillations in Harbours of Arbitrary Shape", W.M. Keck Lab. of Hyd. and Water Resources, Cal. Inst. Tech., Rep. KH-R-20.

Mei, C.C. and Foda, M.A. (1979), "Exact and Hybrid-Element Solution for the Vibration of a Thin Elastic Structure Seated on the Sea Floor", Applied Ocean Research, 1, 79-88.

Werner, P.W. and Sundquist, K.J. (1946), "On Hydrodynamic Earthquake Effects", Trans. Am. Geophys. Union, 30, 636-657.

Westergaard, H.M. (1933), "Water Pressures on Dams During Earthquakes", Trans. ASCE, 98, 418-433.

Zanger, C.N. (1953), "Hydrodynamic Pressures on Dams due to Horizontal Earthquake", Proc. Soc. Exp. Stress Anal., 10, 93-102.

Zanger, C.N. and Haefeli, R.J. (1952), "Electric Analog Indicates Effect of Horizontal Earthquake Shock on Dams", Civil Eng., 22, 278-279.

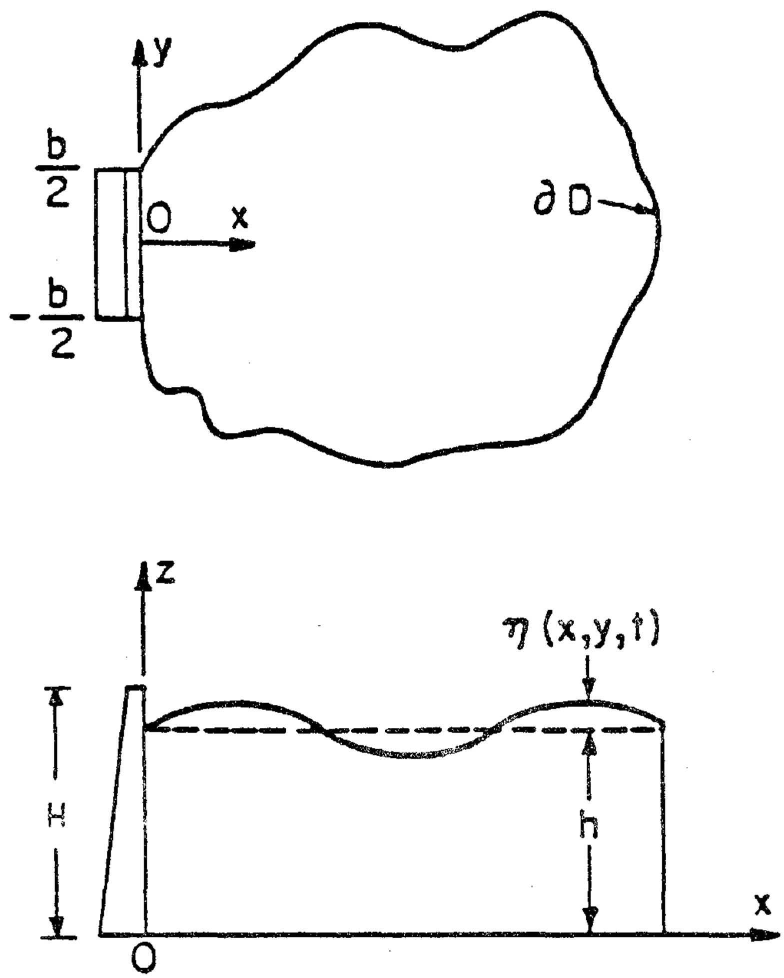

Figure 1. Schematic diagram of an arbitrarily shaped dam-reservoir system.

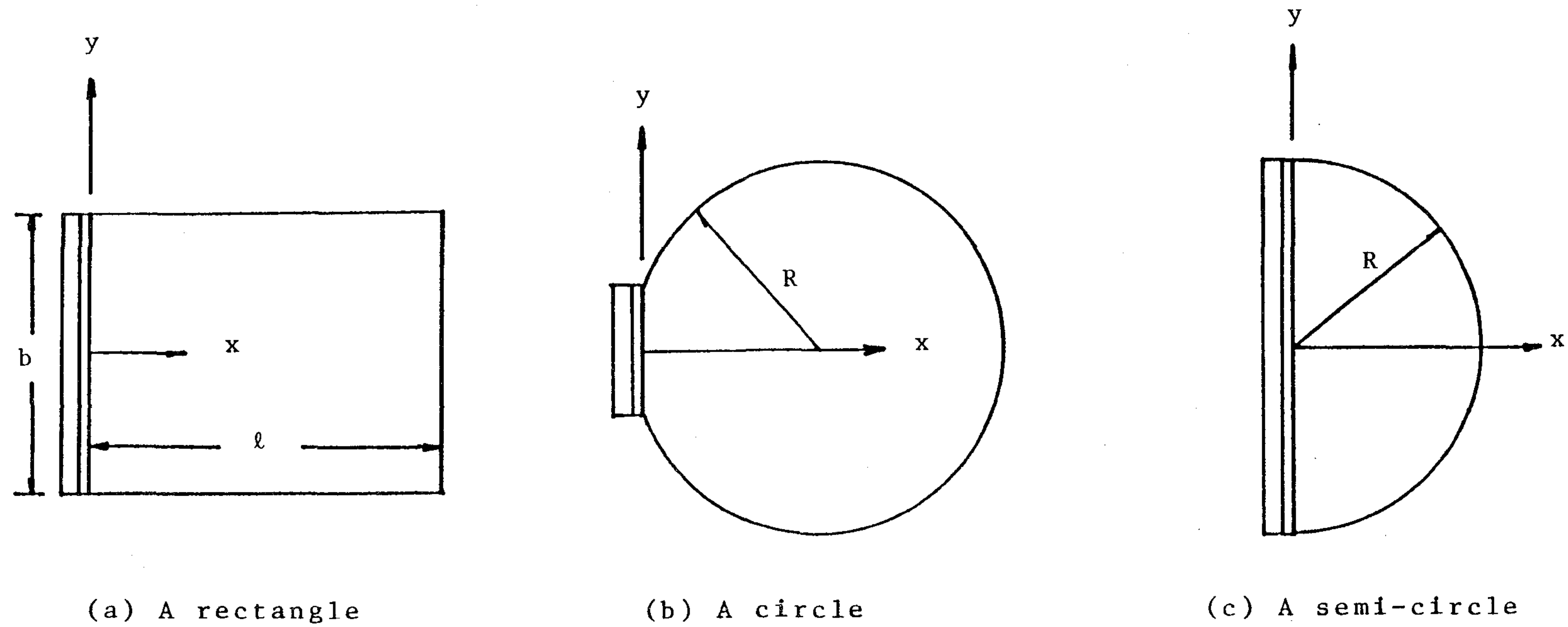

Figure 2. Schematic diagram of a simply shaped dam-reservoir system: (a) A rectangle, (b) A circle, (c) A semi-circle .

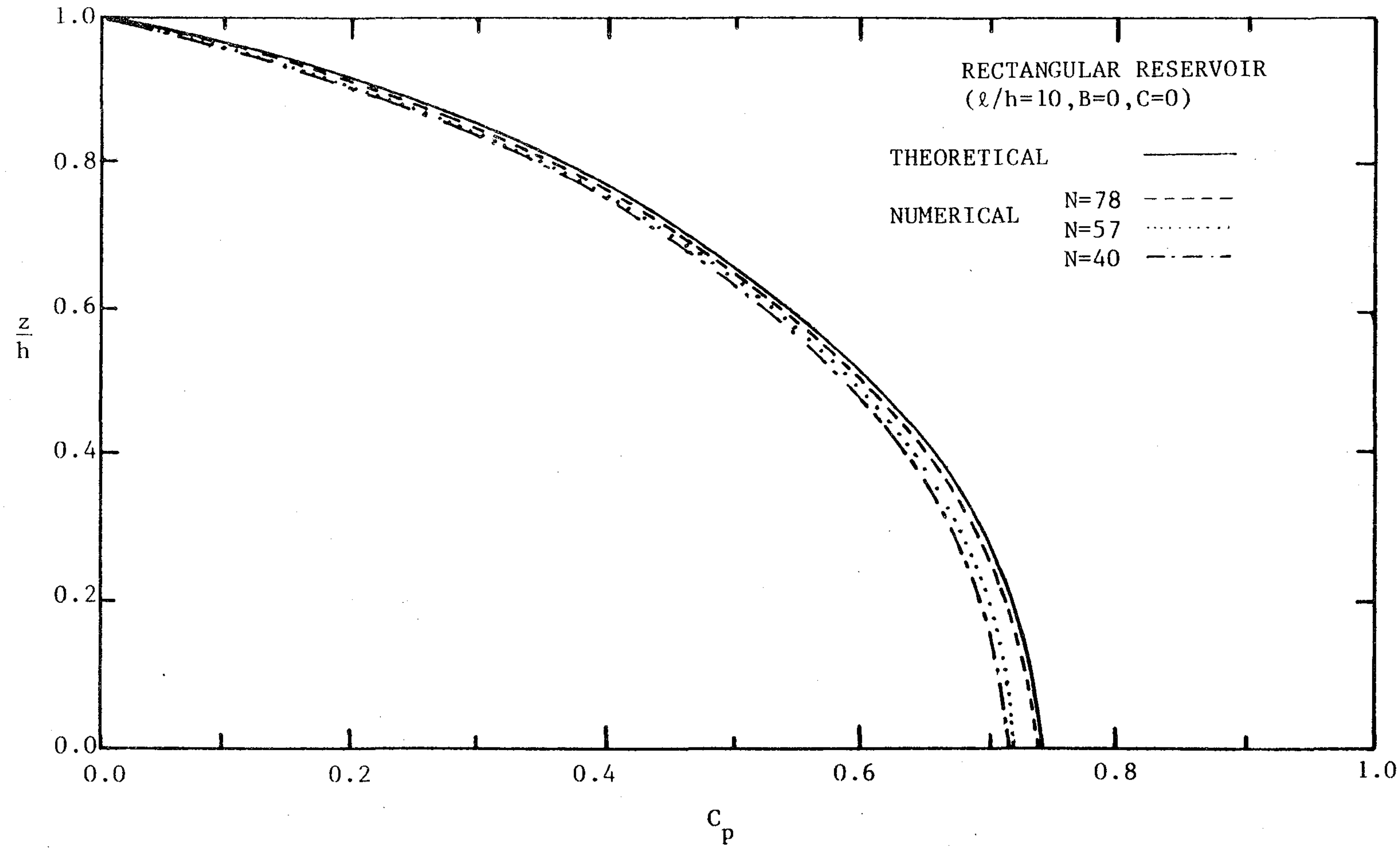

Figure 3. Comparison of the theoretical and numerical results on the pressure coefficient for a rectangular reservoir at different values N with ℓ/h = 10, B = 0 and C = 0.

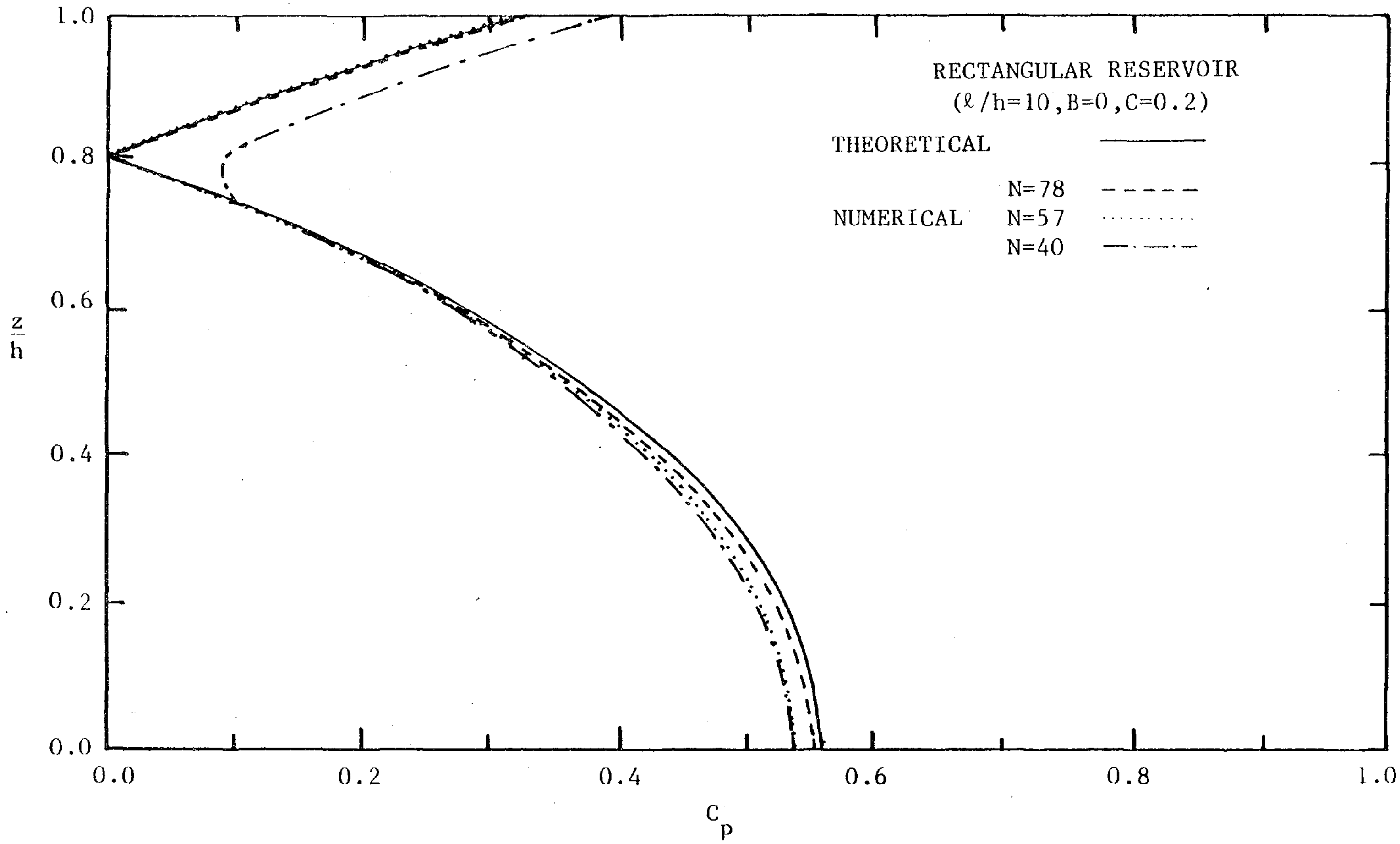

Figure 4. Comparison of the theoretical and numerical results on the pressure coefficient for a rectangular reservoir at different values of N with $\ell/h = 10$, $B = 0$ and $C = 0.2$.

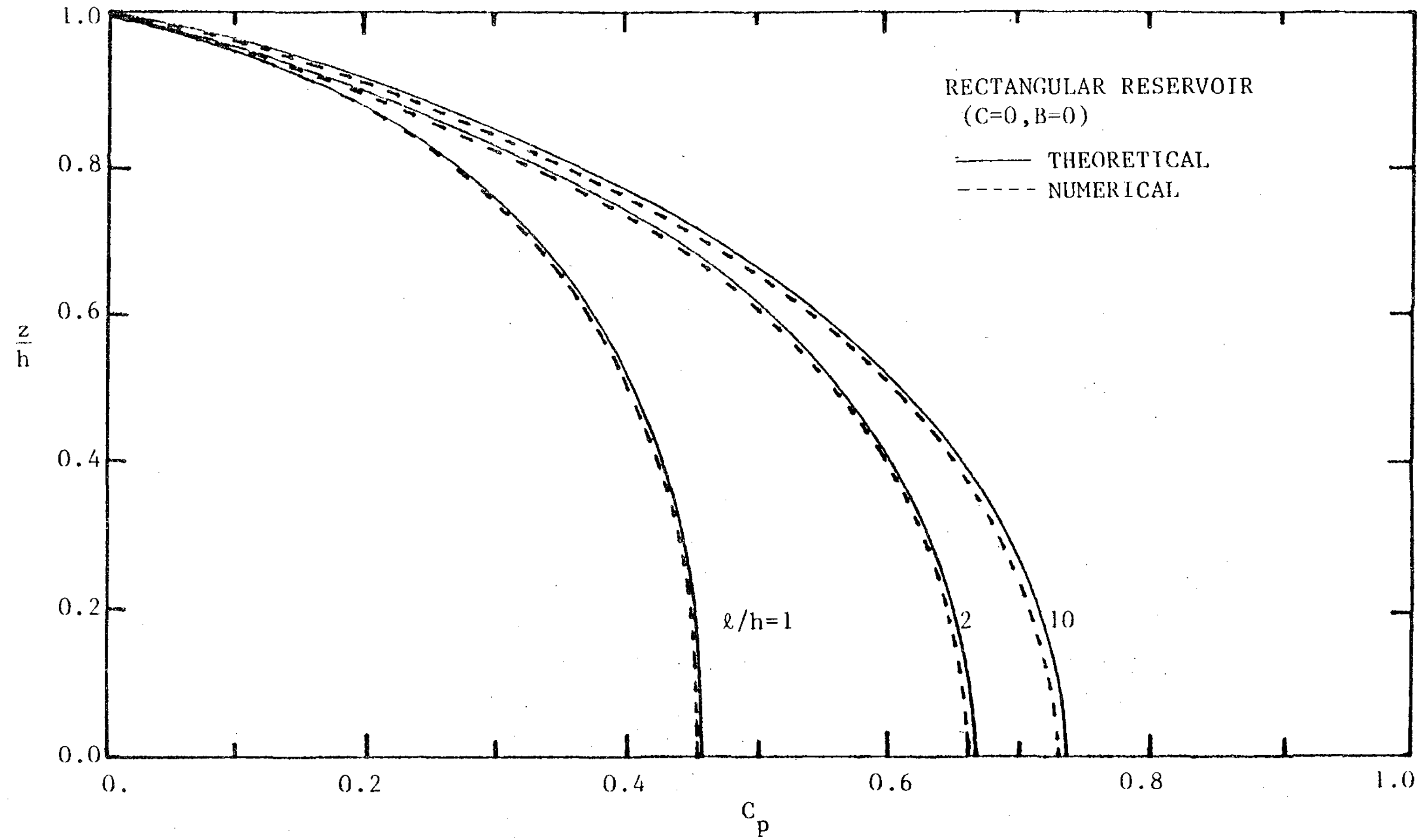

Figure 5. Pressure distribution on a dam for a rectangular reservoir at different values of ℓ/h with C = 0 and B = 0 .

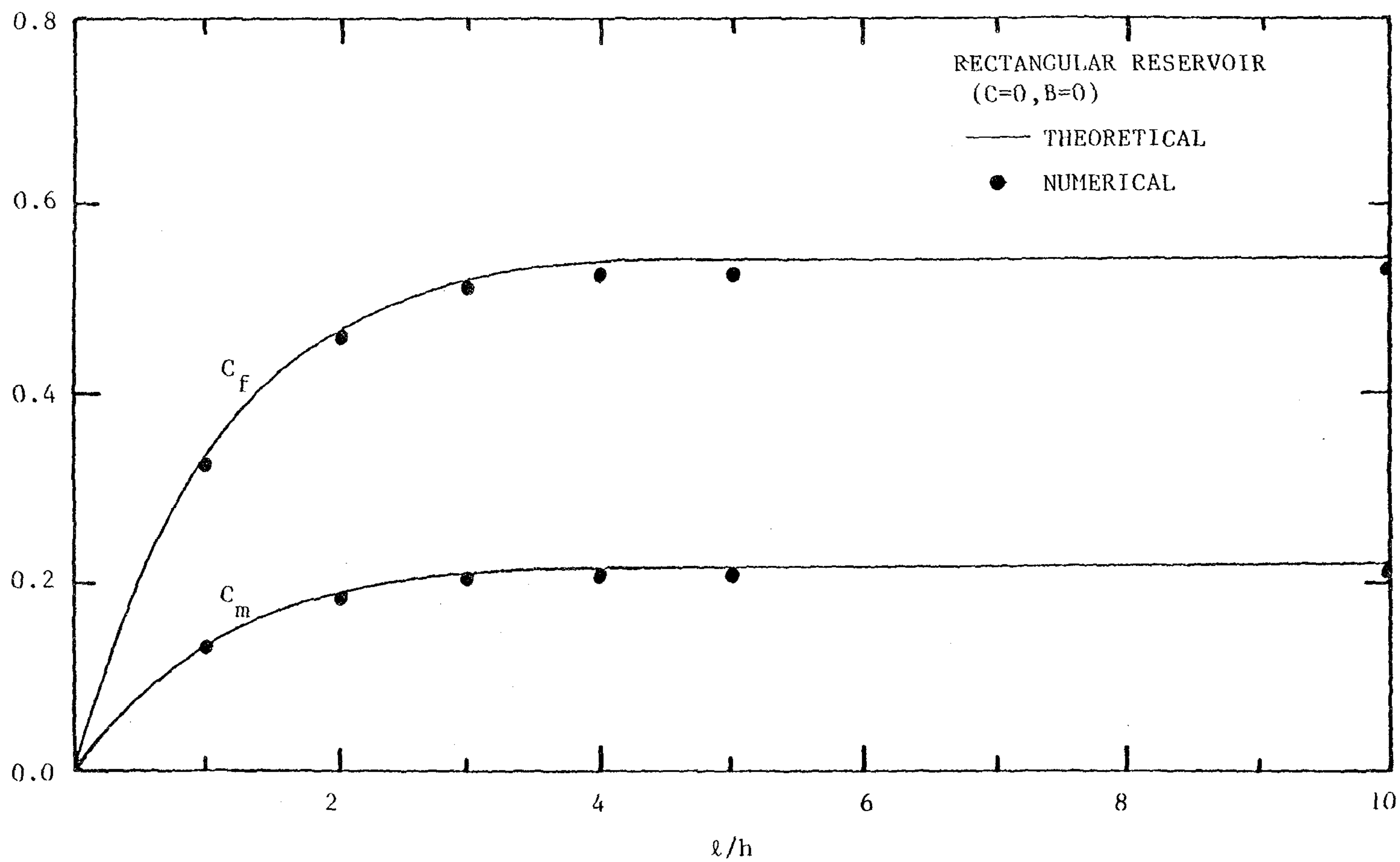

Figure 6. Variation of the force and moment coefficients with ℓ/h for a rectangular reservoir with $C = 0$ and $B = 0$.

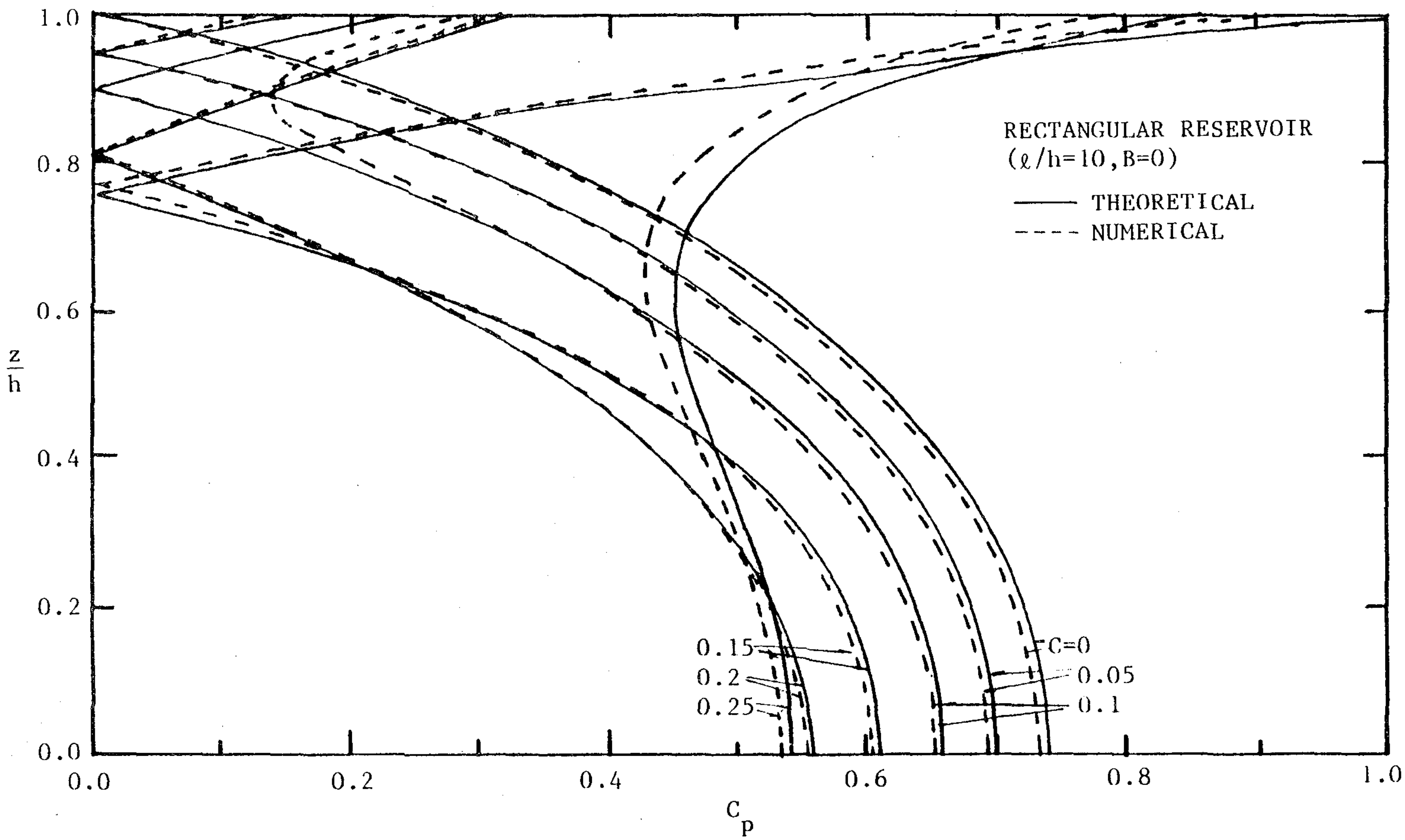

Figure 7. Pressure distribution on a dam for a rectangular reservoir at various values of C with ℓ/h = 10 and B = 0 .

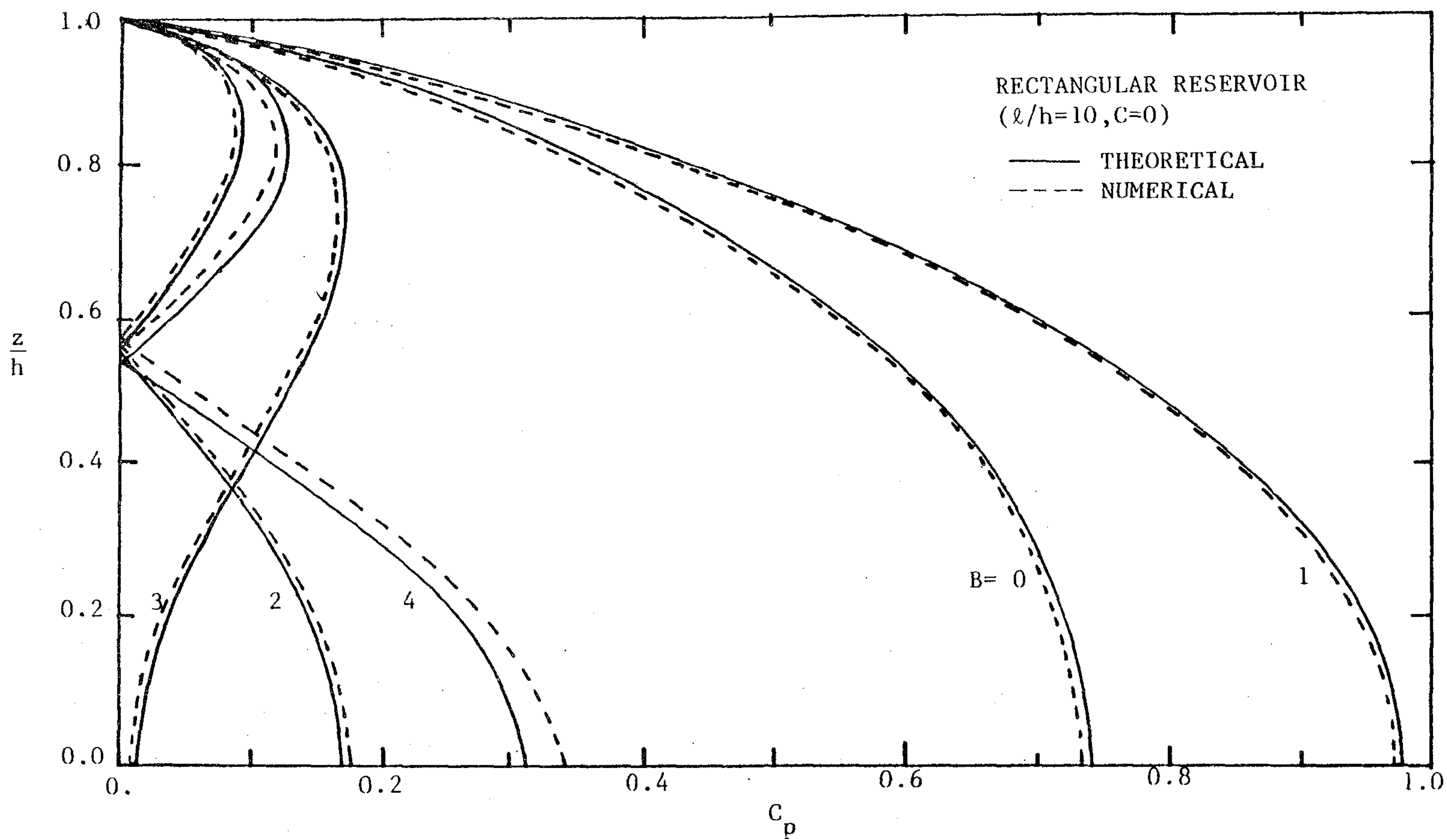

Figure 8. Pressure distribution on a dam for a rectangular reservoir at various values of B with $\ell/h = 10$ and $C = 0$.

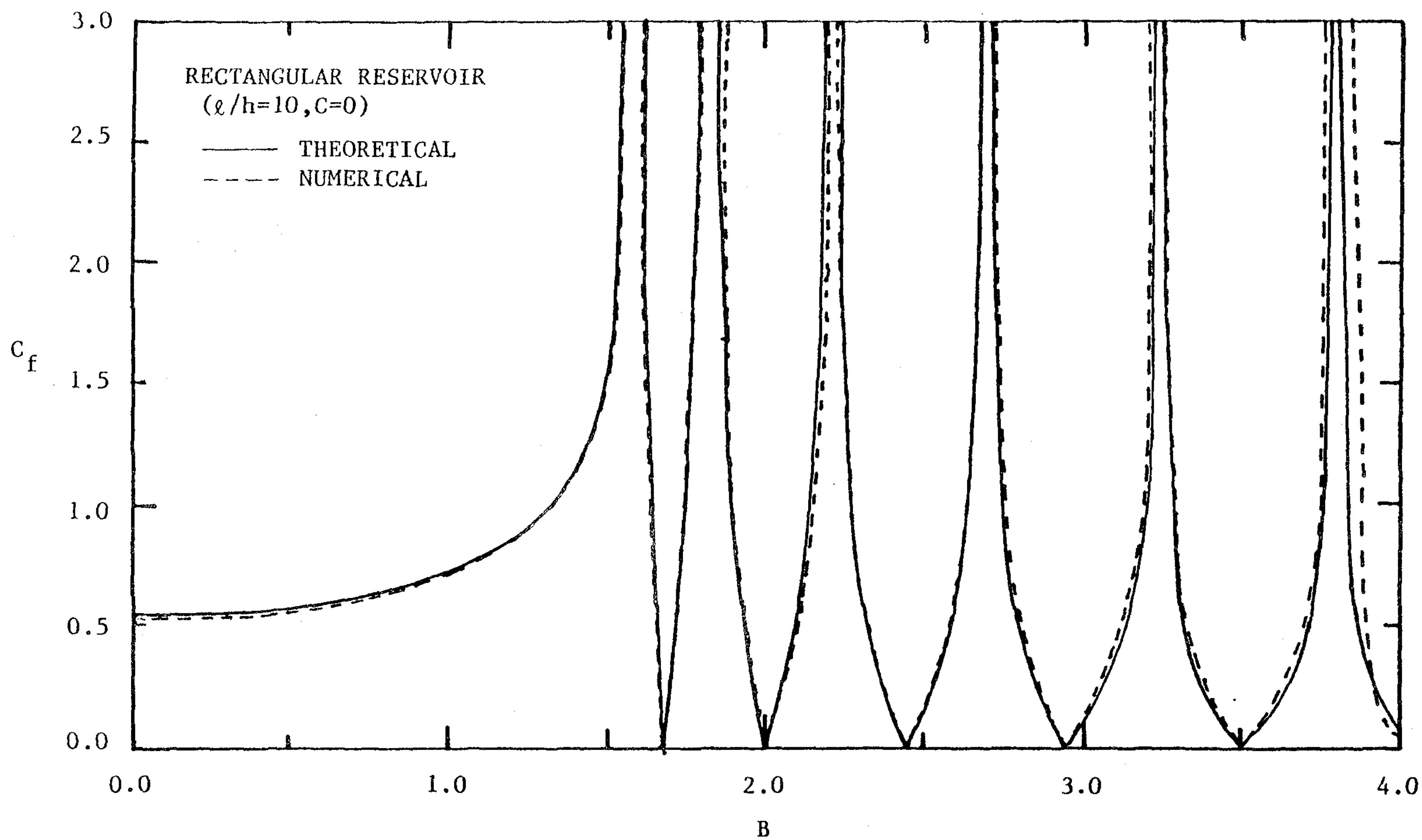

(a) C = 0

Figure 9. Variation of the force coefficient with B for a rectangular reservoir with $\ell/h = 10$: (a) C = 0, (b) C = 0.05.

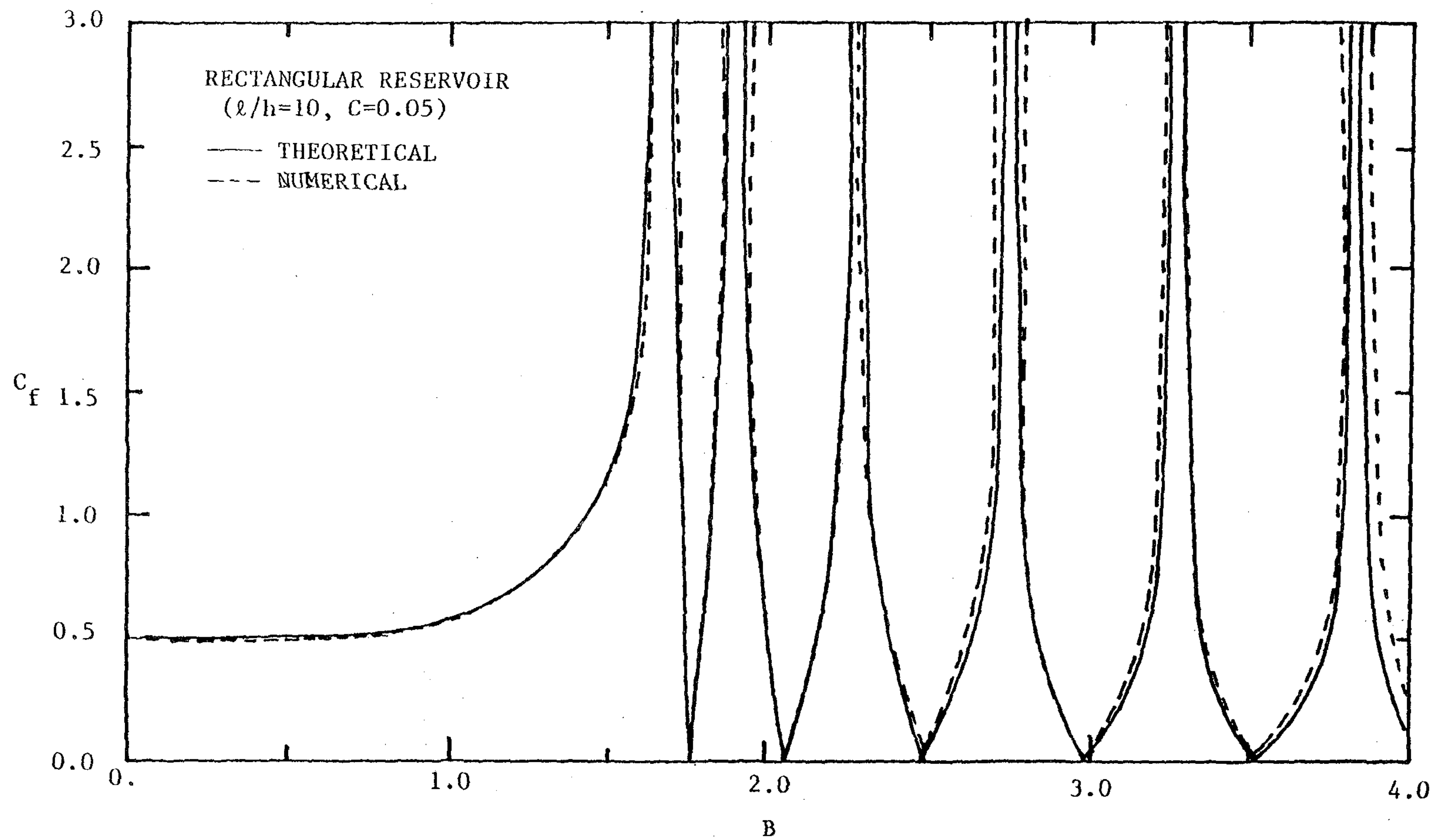

(b) C = 0.05

Figure 9. (Continued)

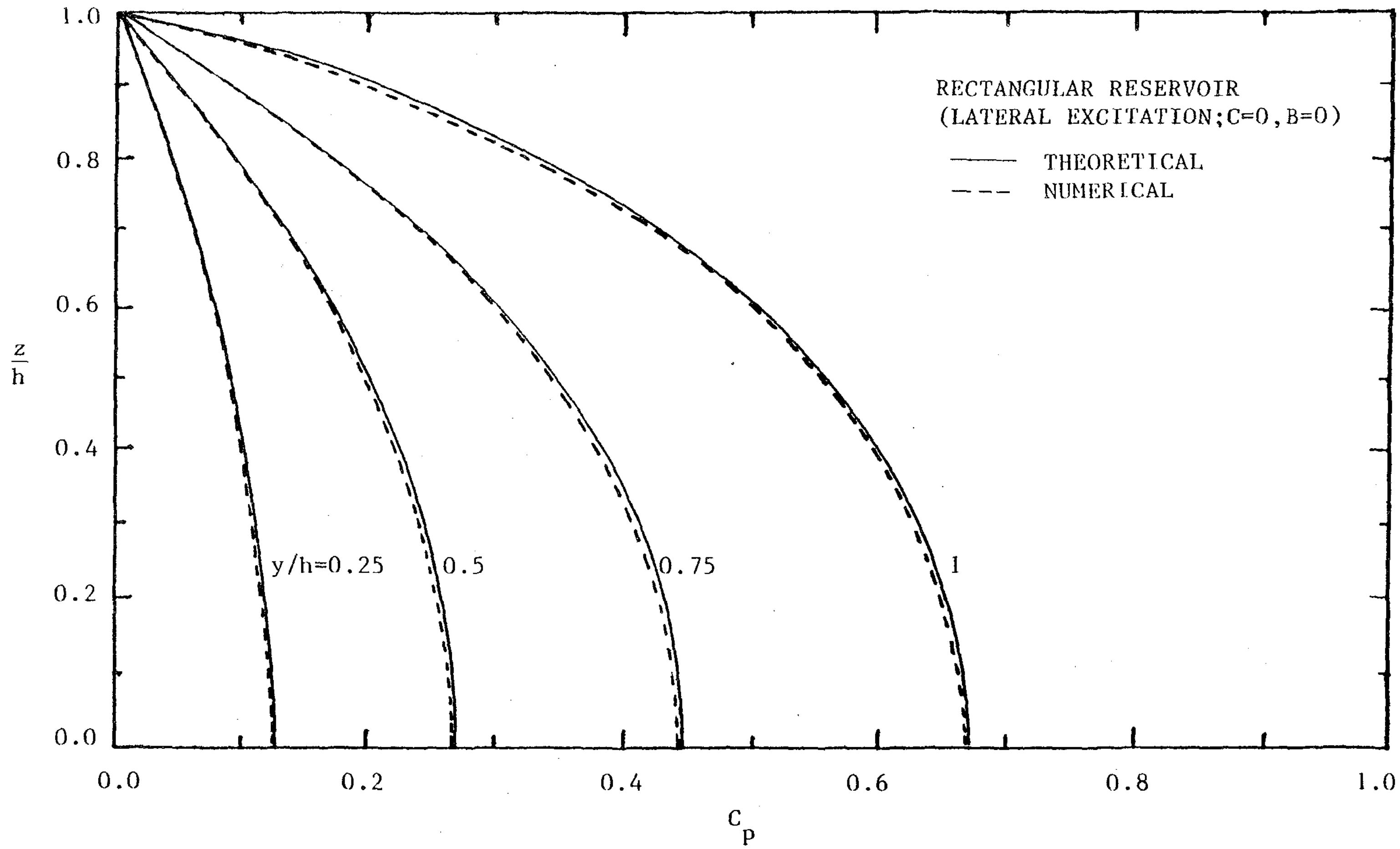

Figure 10. Pressure distribution on a dam at different y/h for a rectangular reservoir due to a lateral excitation with $b/h = 2$, $\ell/h = 10$, $C = 0$ and $B = 0$.

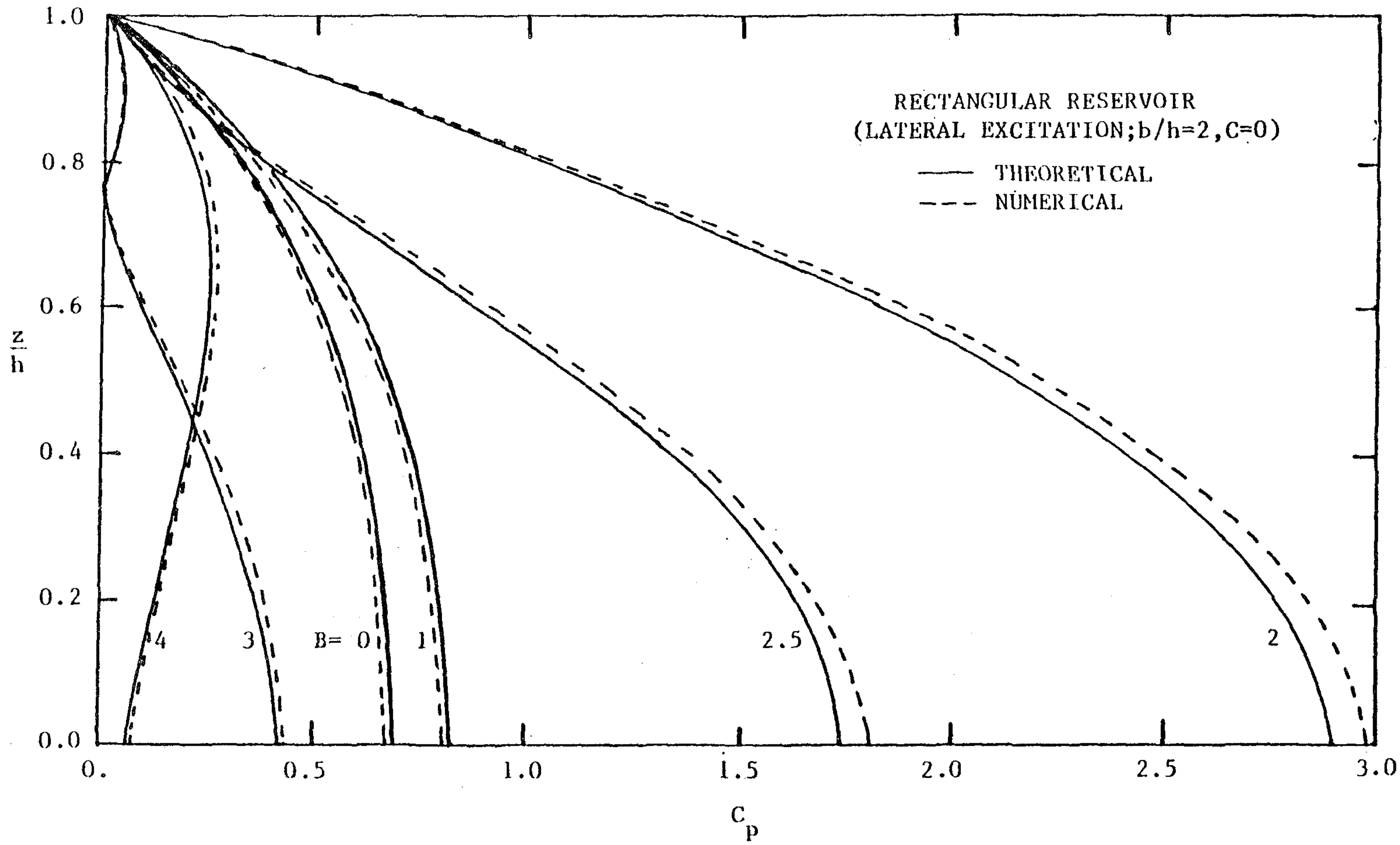

Figure 11. Pressure distribution on a dam at y/h = 1 for a rectangular reservoir at various values of B due to a lateral excitation with b/h = 2, ℓ/h = 10 and C = 0.

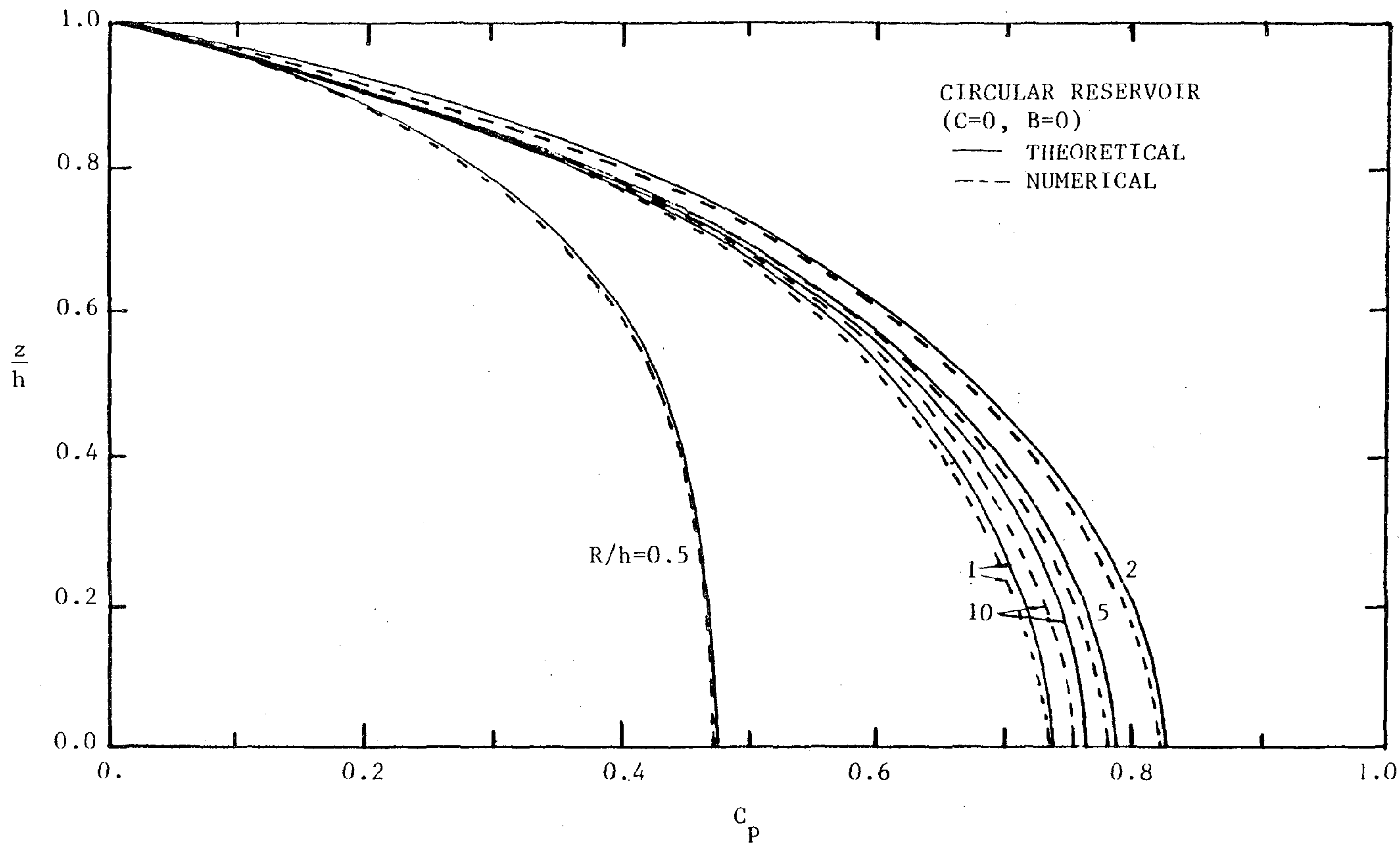

Figure 12. Pressure distribution on a dam for a circular reservoir at various values of R/h with C = 0 and B = 0.

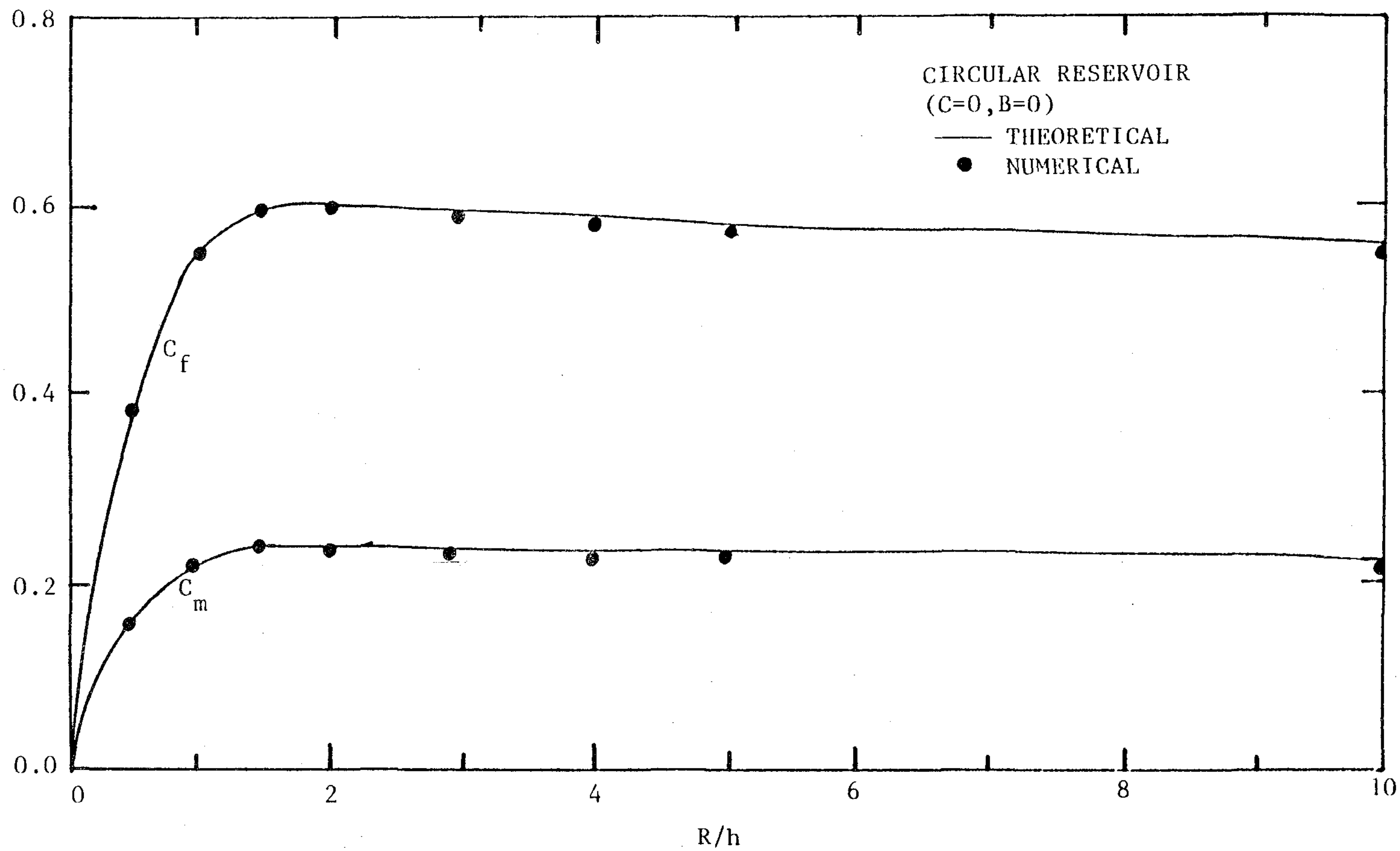

Figure 13. Variation of the force and moment coefficients with R/h for a circular reservoir at C = 0 and B = 0.

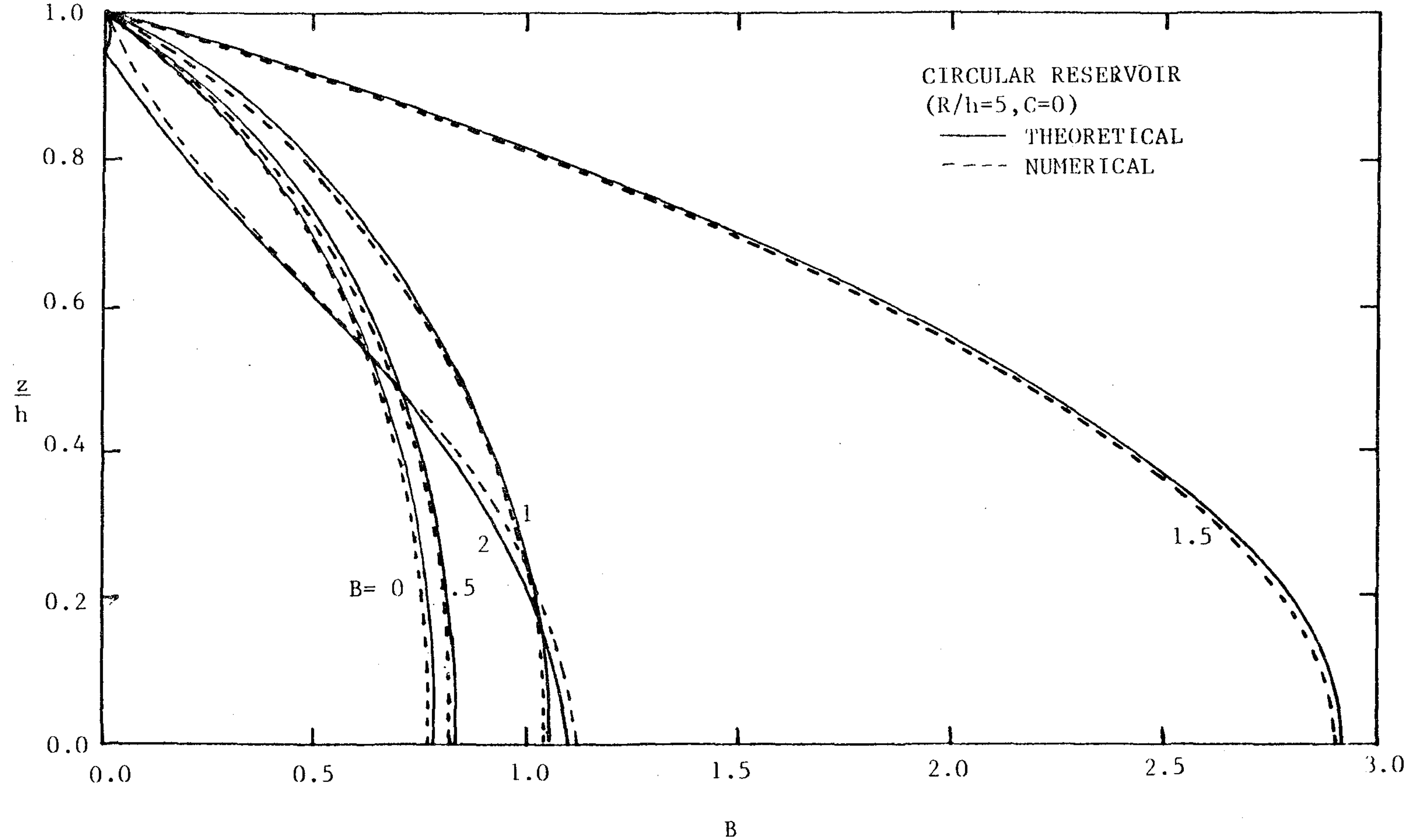

Figure 14. Pressure distribution on a dam for a circular reservoir at various values of B with R/h = 5 and C = 0.

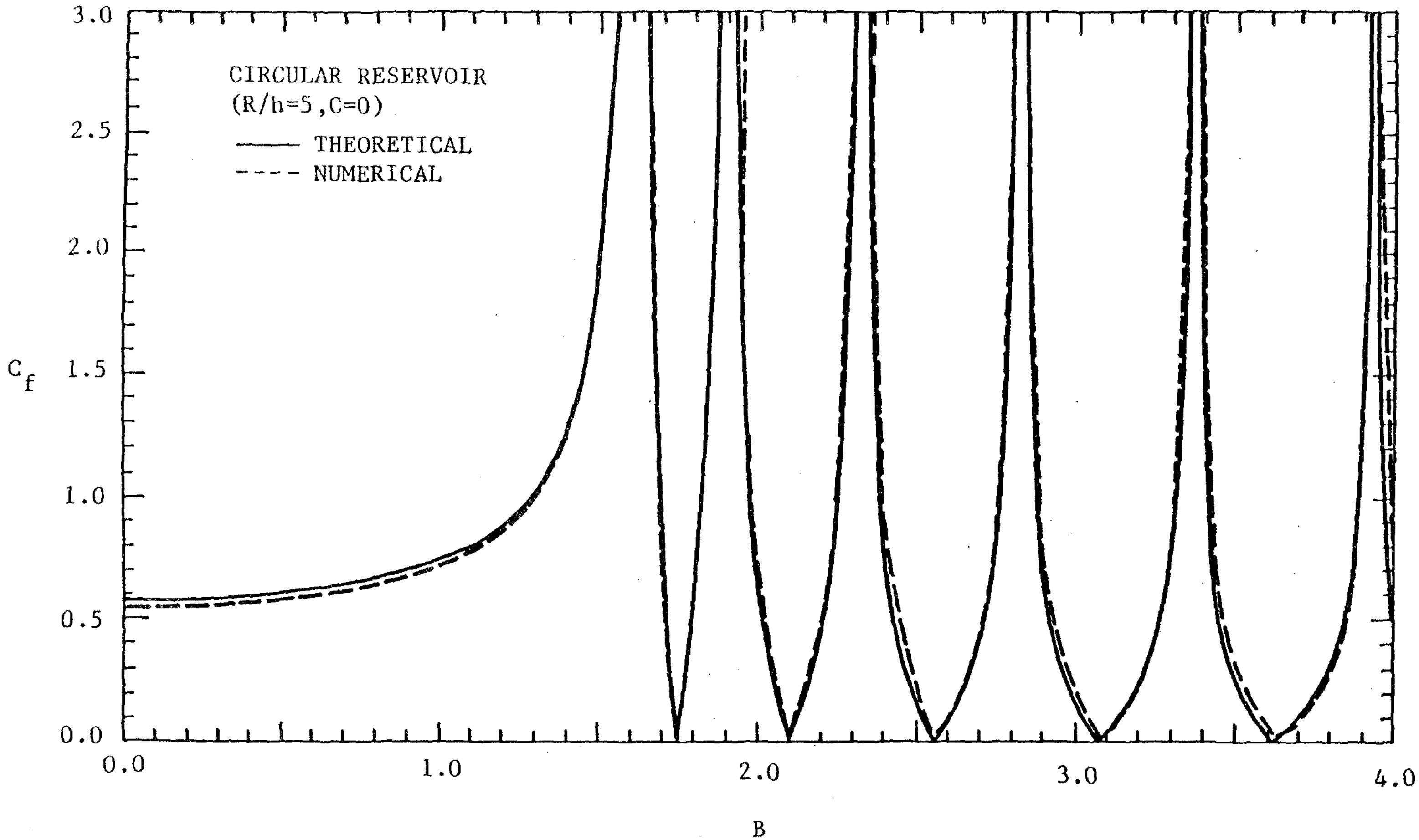

(a) C = 0

Figure 15. Variation of the force coefficient with B for a circular reservoir at R/h = 5: (a) C = 0, (b) C = 0.05 .

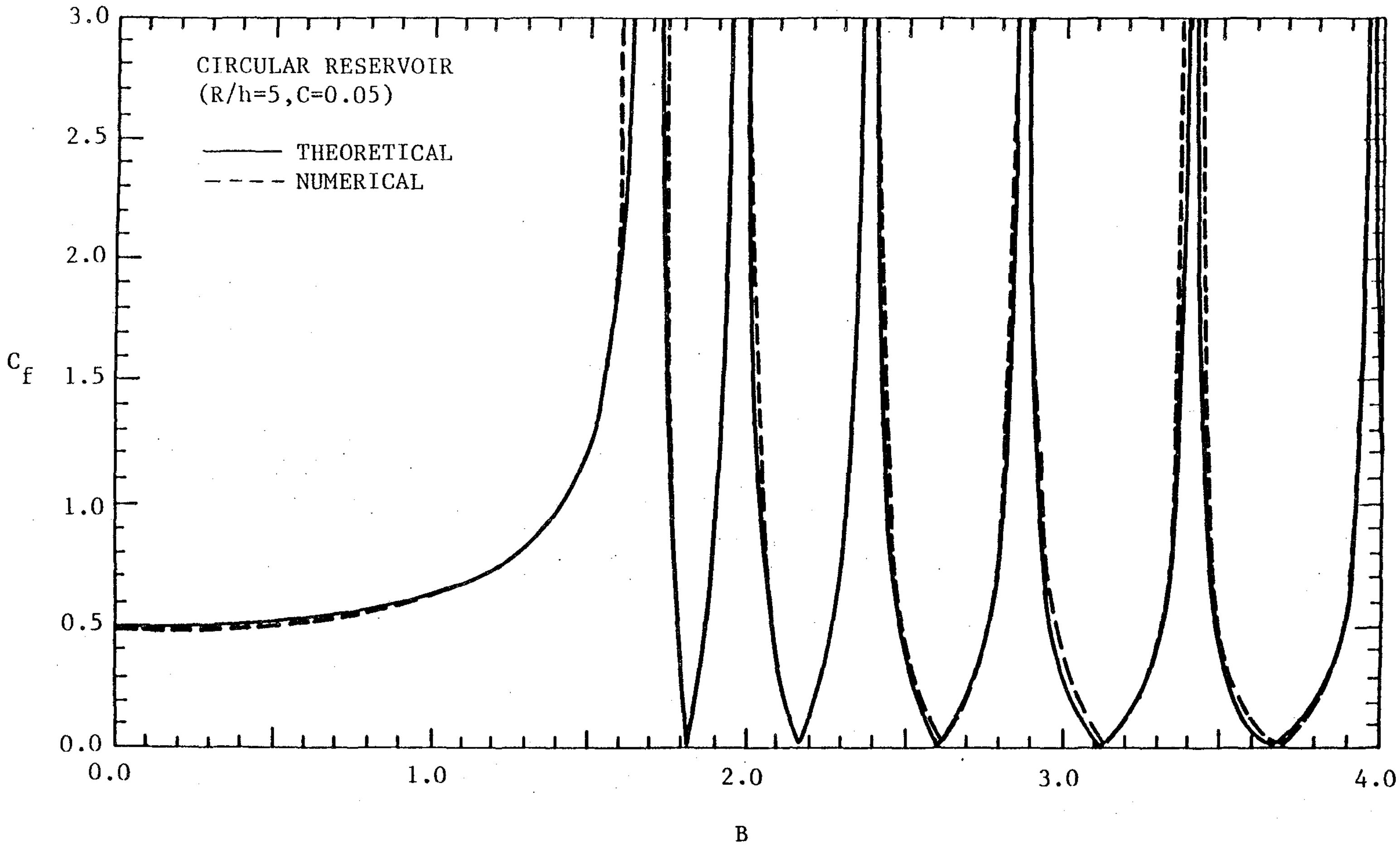

(b) C = 0.05

Figure 15. (Continued)

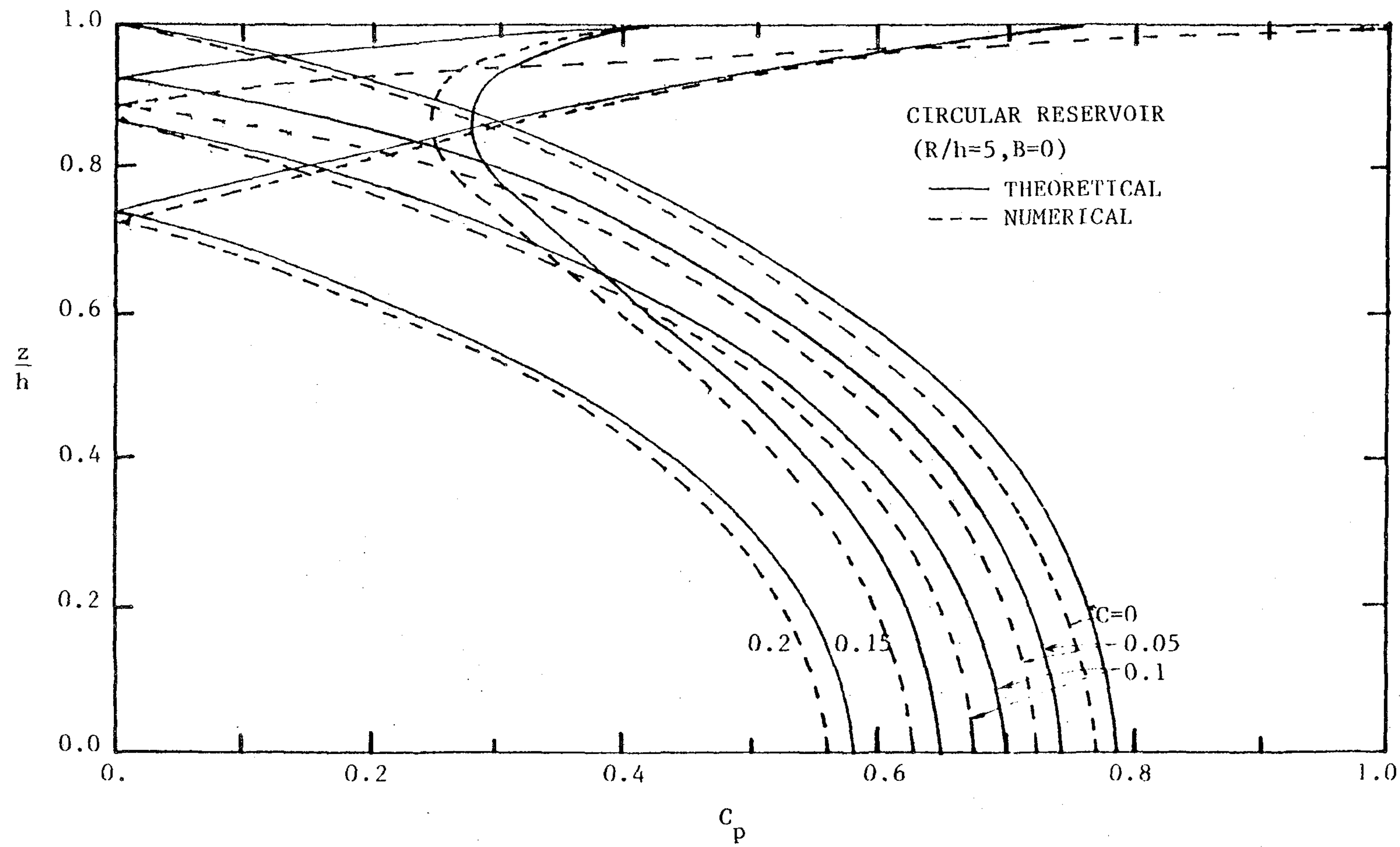

Figure 16. Pressure distribution on a dam for a circular reservoir at various values of C with R/h = 5 and B = 0 .

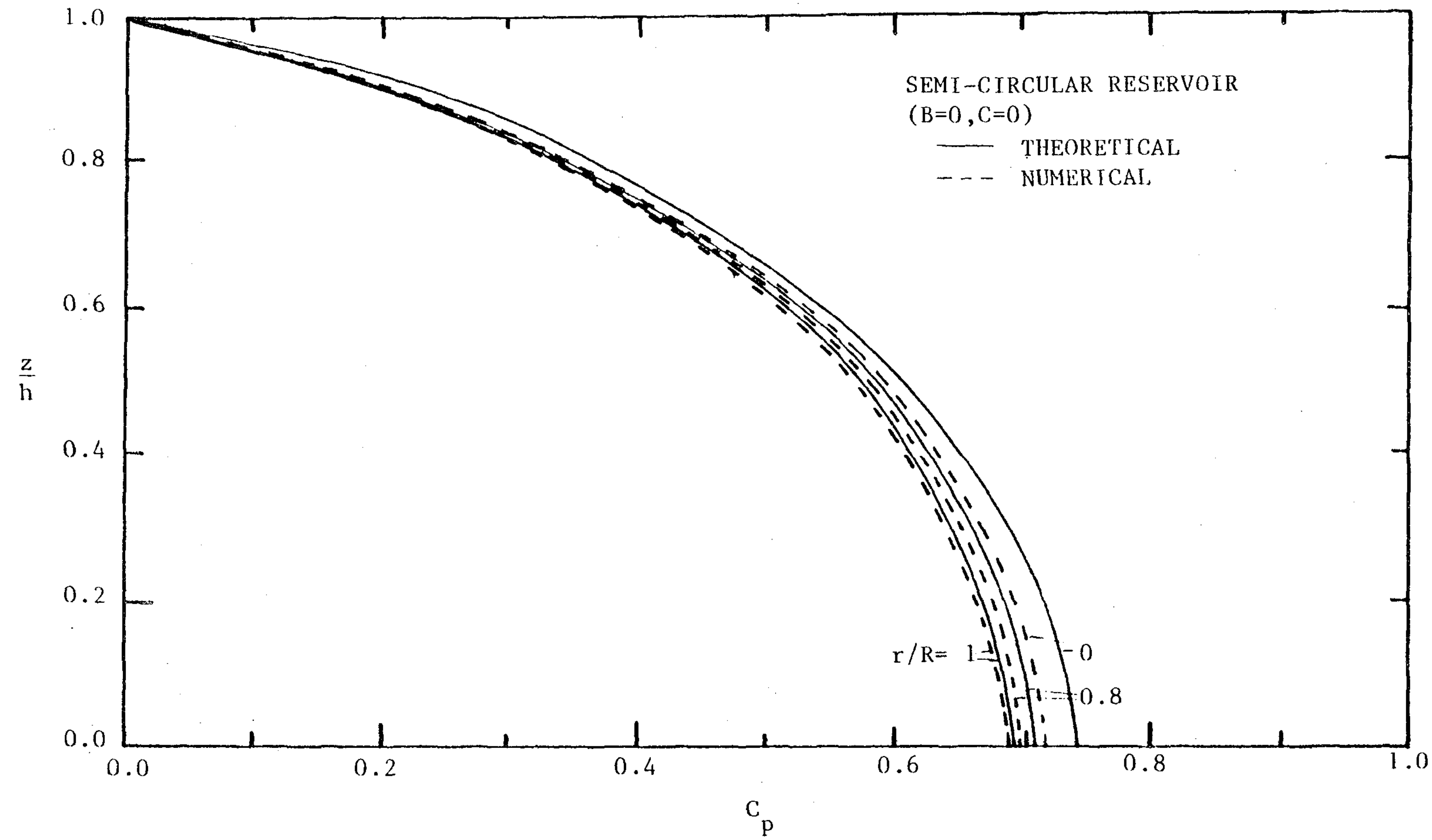

Figure 17. Pressure distribution on a dam for a semi-circular reservoir at different values of r/R with R/h = 5, B = 0 and C = 0.

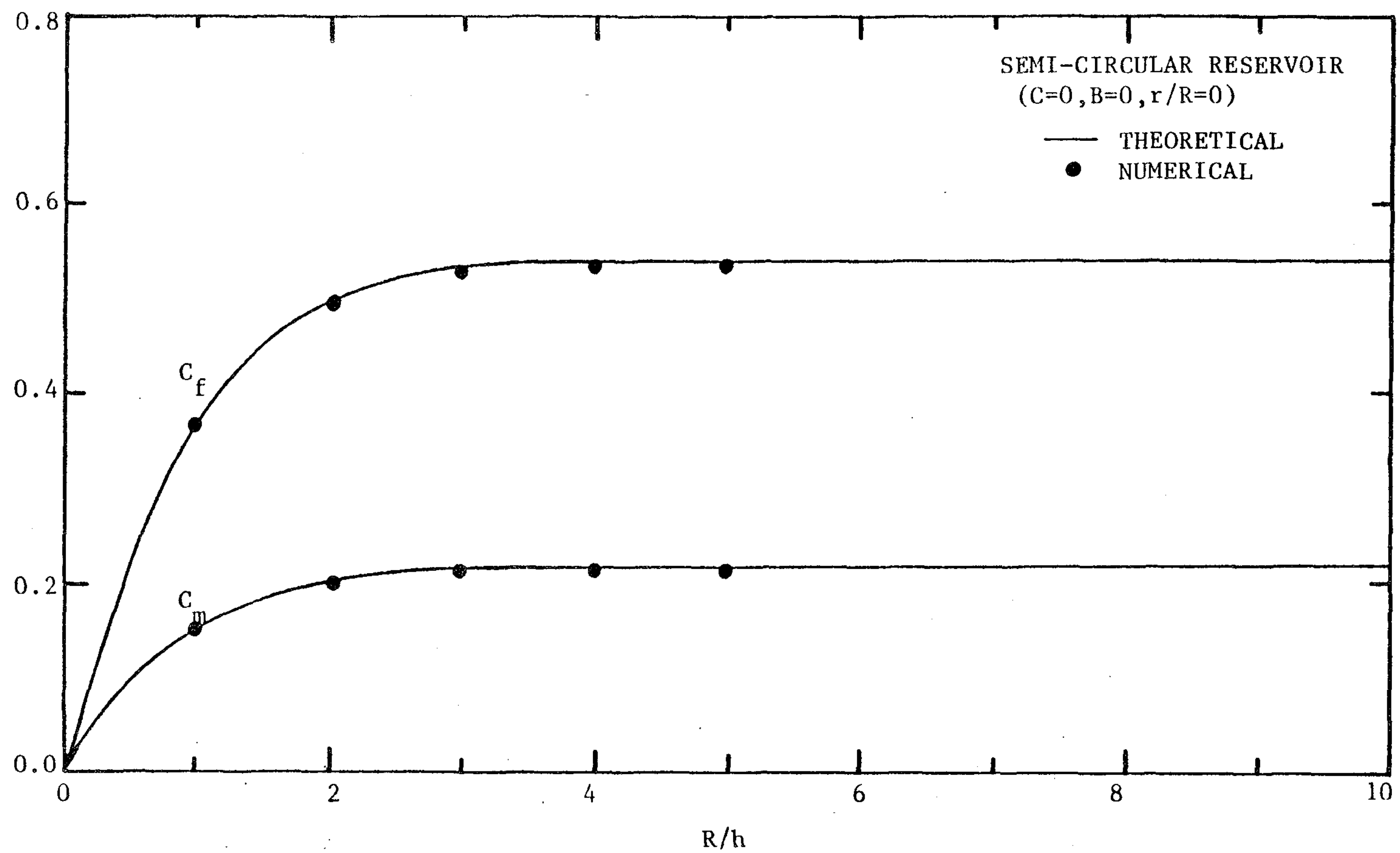

Figure 18. Variation of the force and moment coefficients with R/h for a semi-circular reservoir at C = 0, B = 0 and r/R = 0.

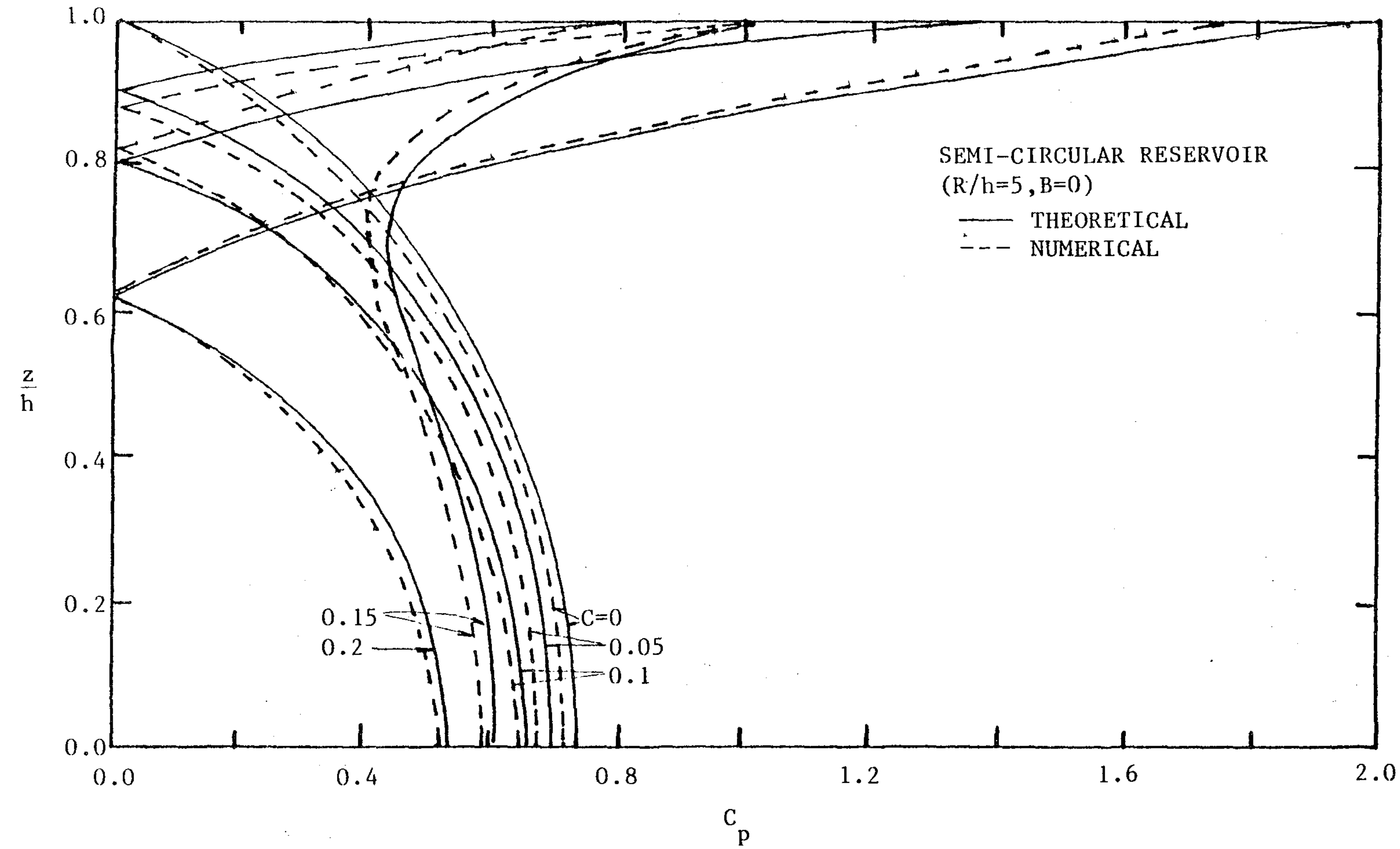

Figure 19. Pressure distribution at the center of a dam for a semi-circular reservoir at various values of C with R/h = 5 and B = 0.

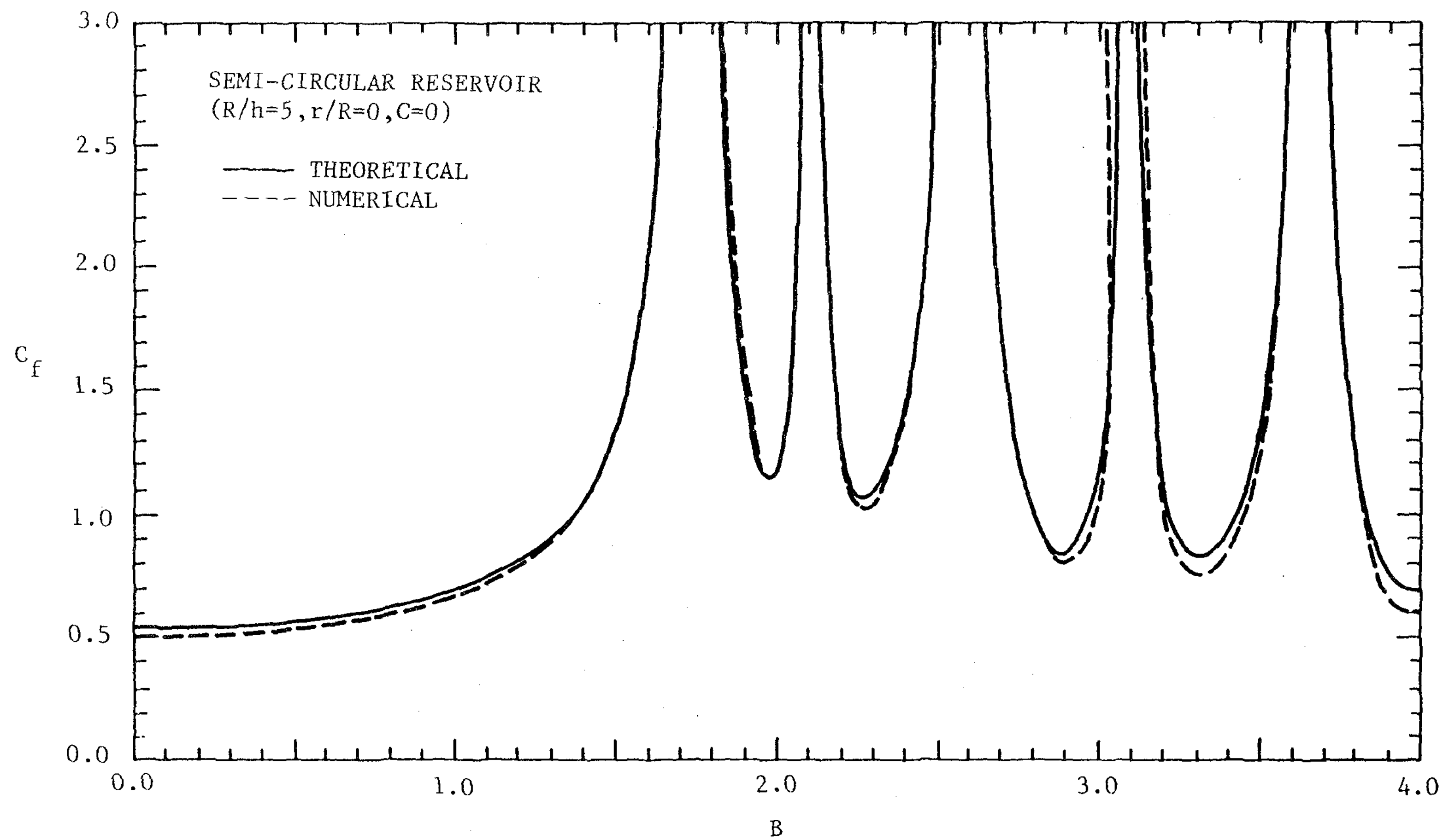

(a) C = 0

Figure 20. Variation of the force coefficient with B for a semi-circular reservoir at $r/R = 0$ and $R/h = 5$: (a) $C = 0$, (b) $C = 0.05$.

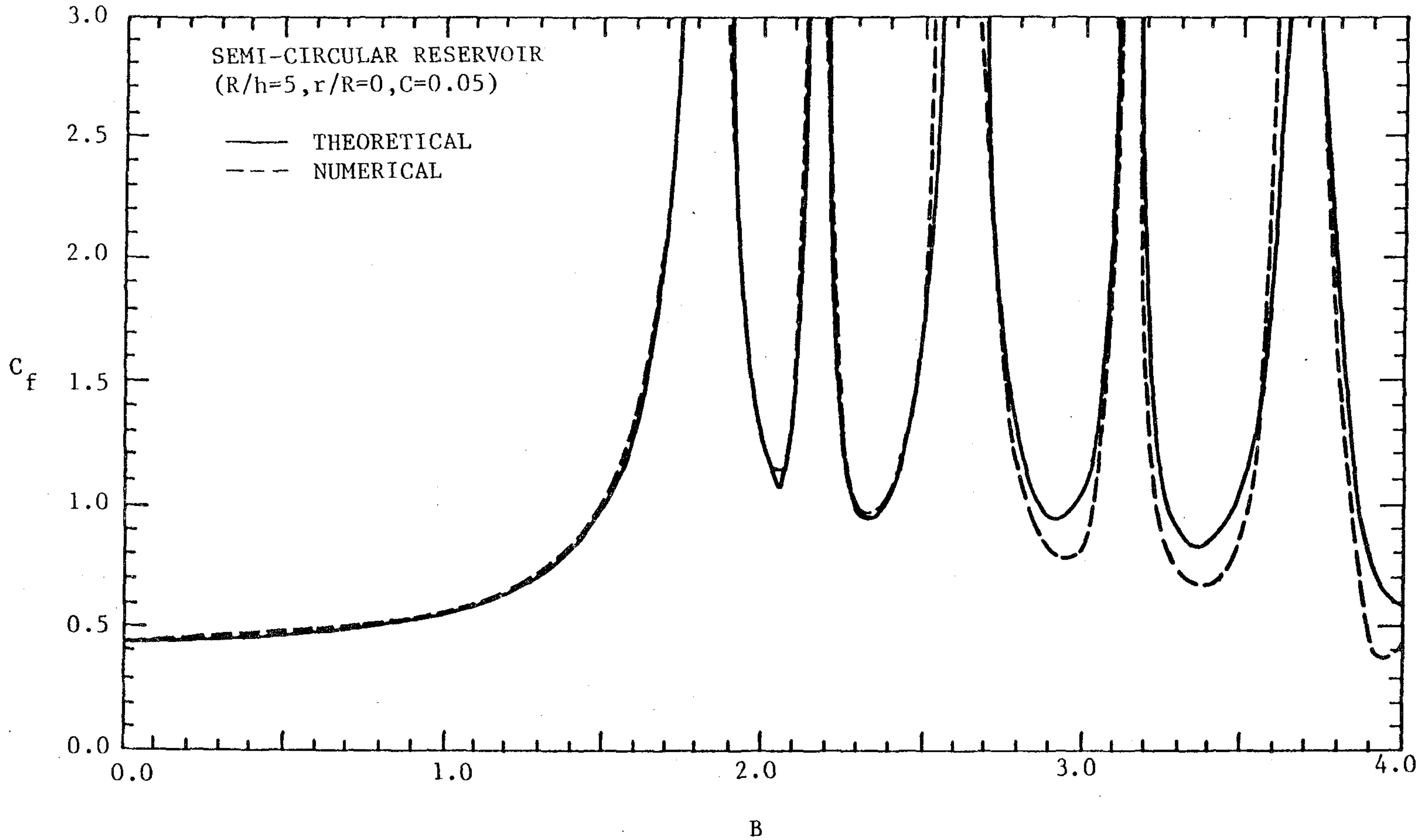

(b) C = 0.05

Figure 20. (Continued)

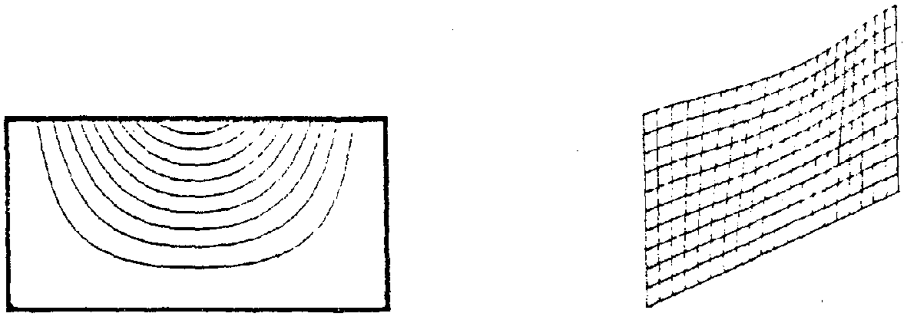

(i) First mode (λ^2 = 32.07)

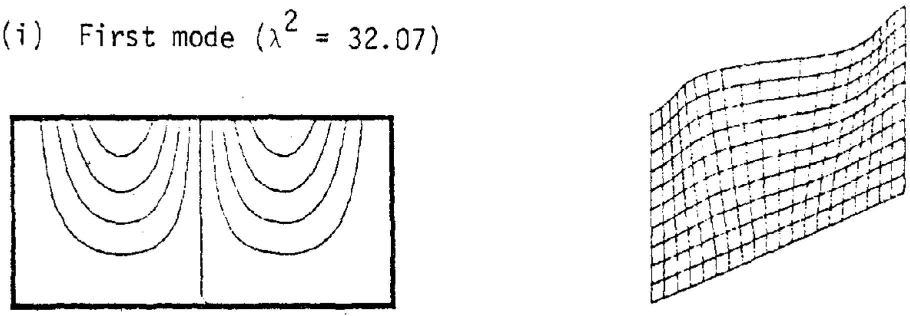

(ii) Second mode (λ^2 = 71.59)

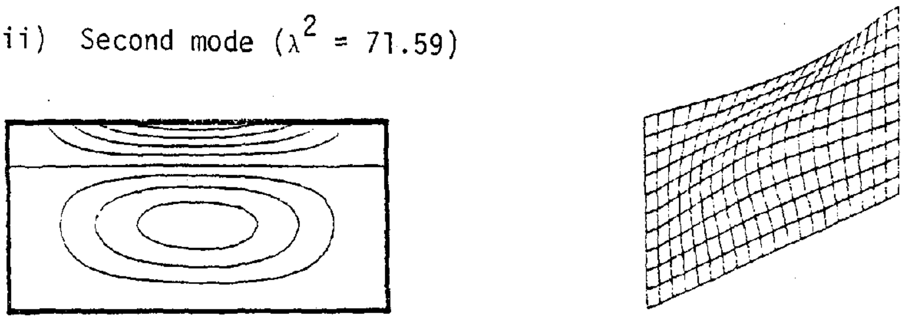

(iii) Third mode (λ^2 = 104.41)

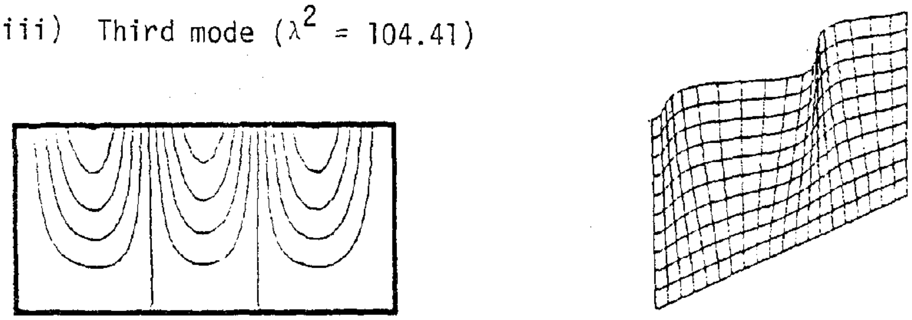

(iv) Fourth mode (λ^2 = 130.62)

(a) b/h = 2

Figure 21. Normal mode shapes of a rectangular plate with (a) b/h = 2, (b) b/h = 10.

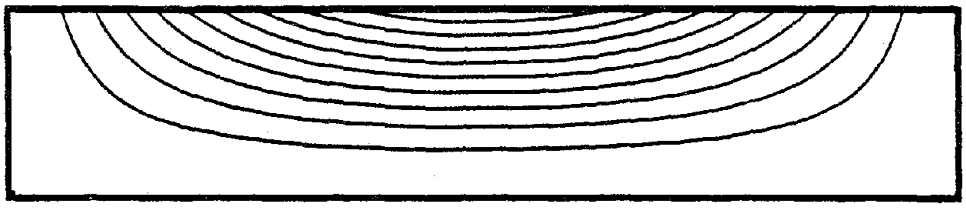

(i) First mode (λ^2 = 363.62)

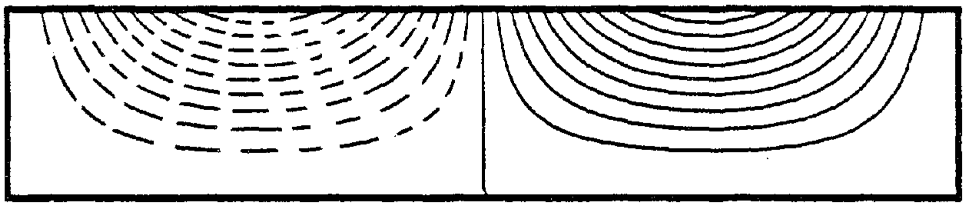

(ii) Second mode (λ^2 = 398.88)

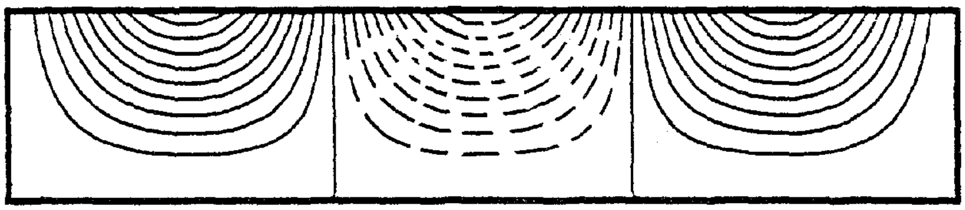

(iii) Third mode (λ^2 = 455.52)

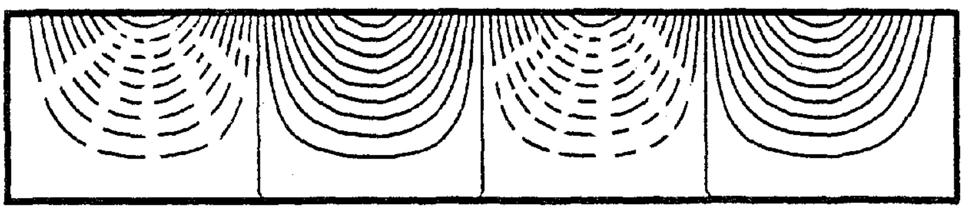

(iv) Fourth mode (λ^2 = 532.11)

(b) b/h = 10

Figure 21. (Continued)

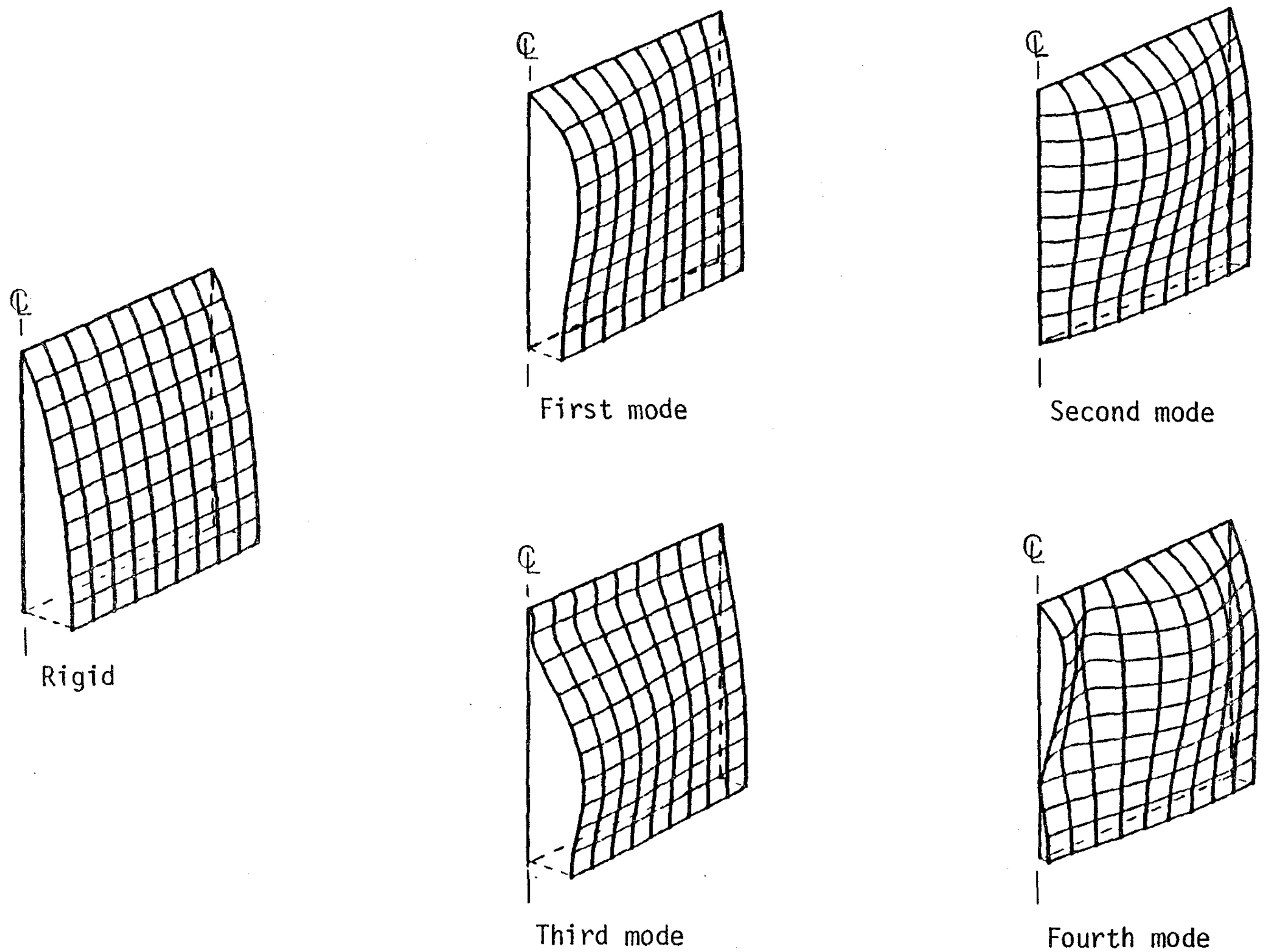

(a) A rectangular reservoir with $b/h = 2$, $\ell/h = 10$, $C = 0$ and $B = 1$

Figure 22. Pressure distributions on a dam for each mode .

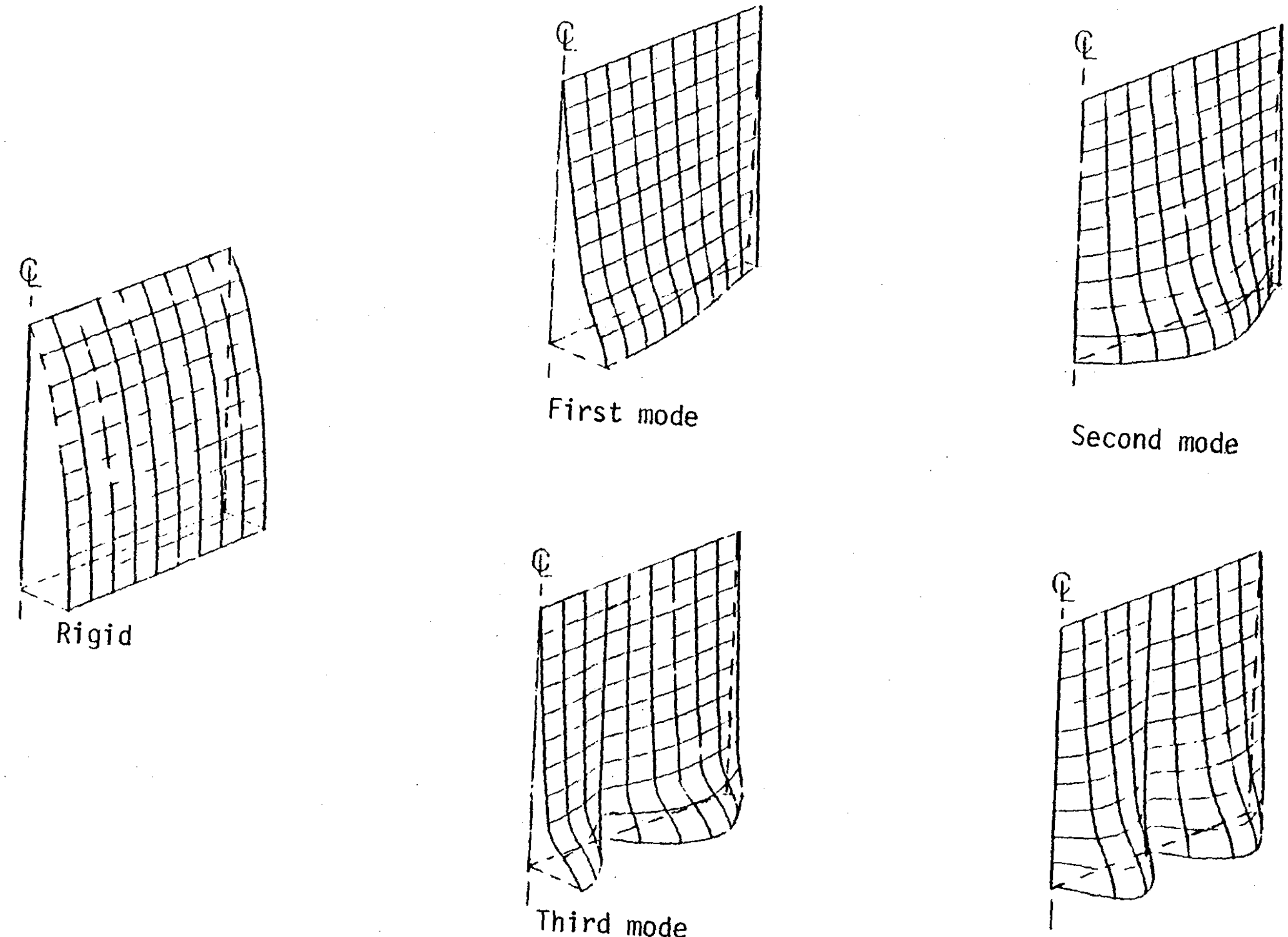

(b) A semi-circular reservoir with $b/h = 10$, $R/h = 5$, $C = 0$ and $B = 1$

Figure 22. (Continued)

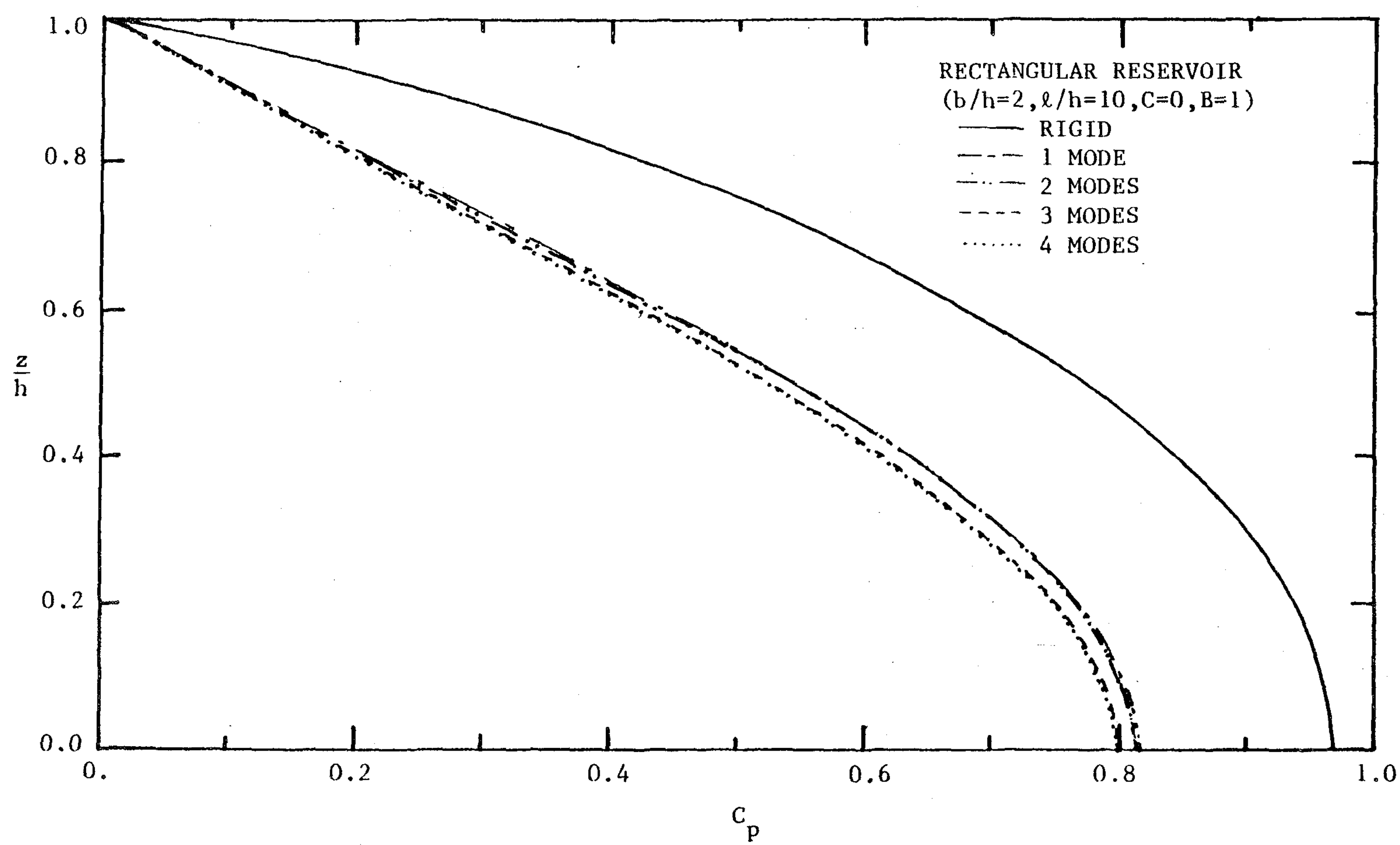

Figure 23. Comparison between the pressure distributions due to different numbers of modes with $b/h = 2$, $\ell/h = 10$, $C = 0$ and $B = 1$.

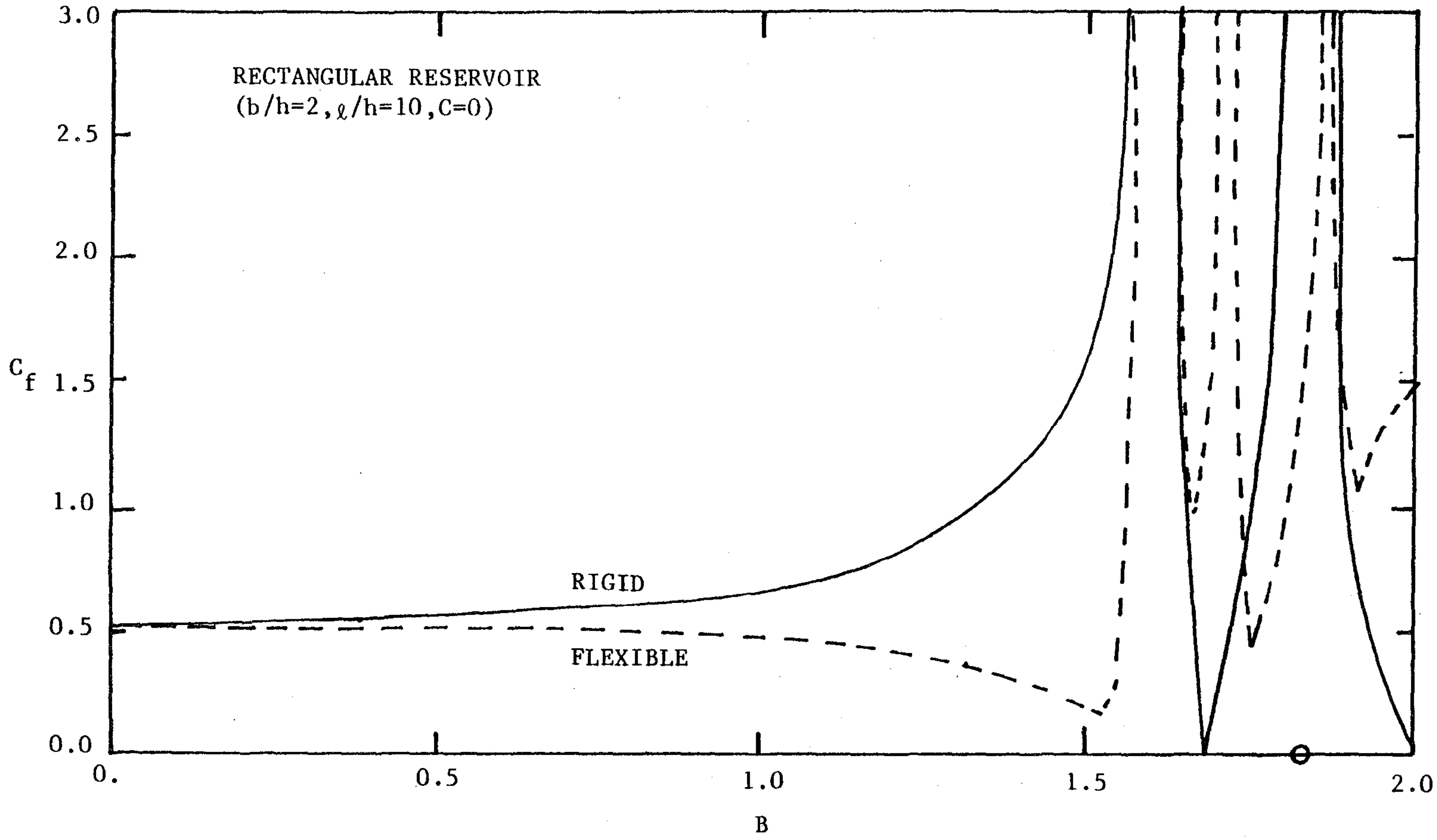

Figure 24. Hydrodynamic force response for a rectangular reservoir with $b/h = 2$, $\ell/h = 10$ and $C = 0$. (The open circle on the abscissa denotes the natural frequency of the dam only).

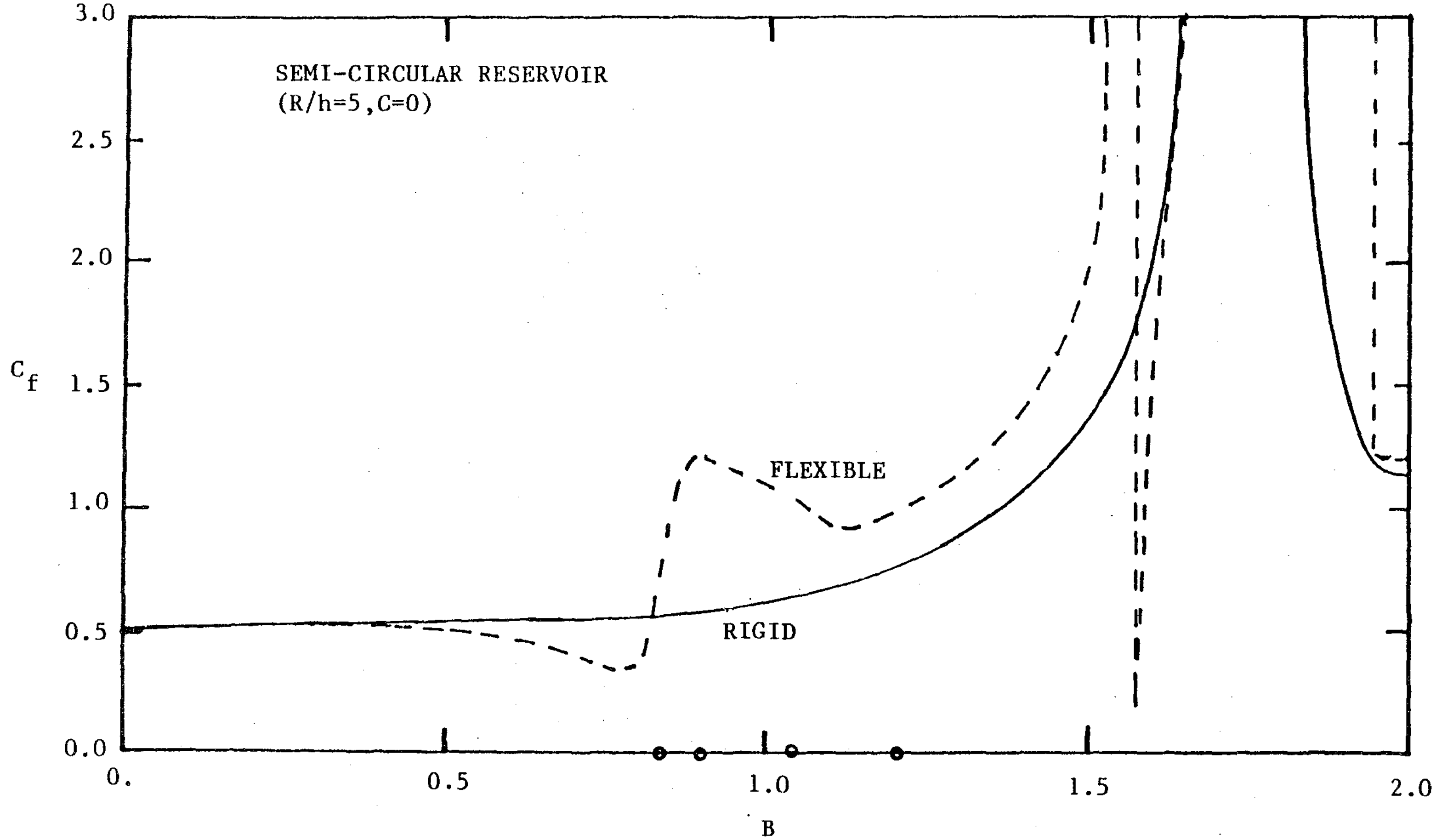

Figure 25. Hydrodynamic force response for a semi-circular reservoir with R/h = 5 and C = 0. (The open circles on the abscissa denote natural frequencies of the dam only).

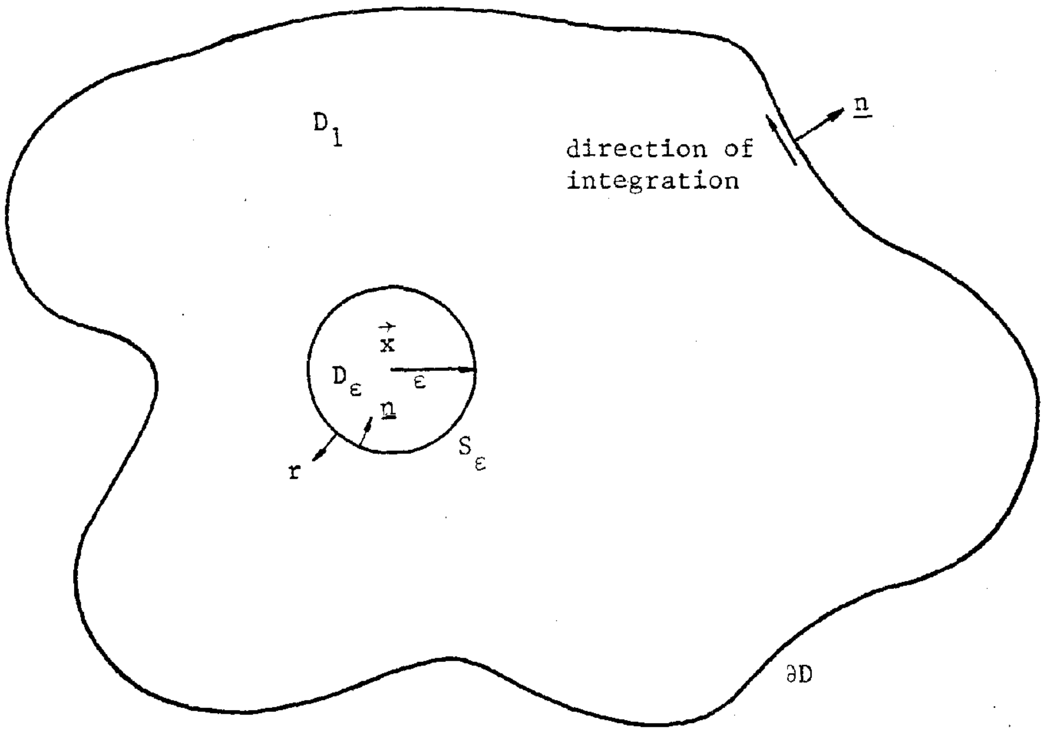

Figure A.1. Definition sketch for a bounded domain.

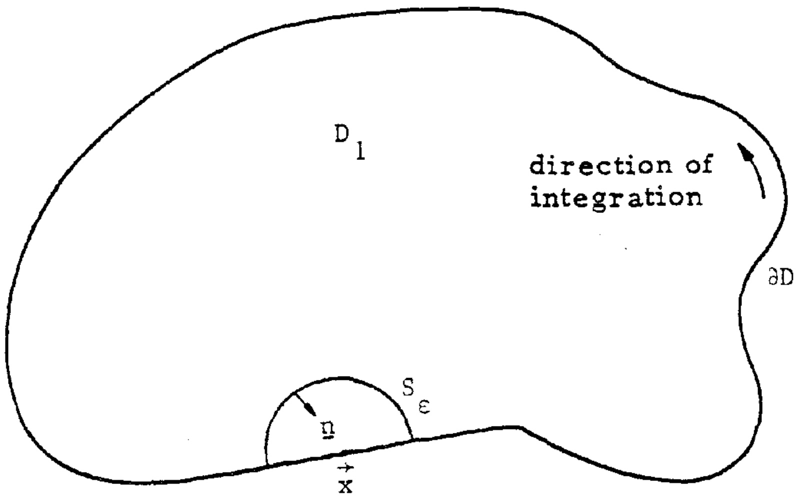

Figure A.2. Definition sketch for an interior point approaching a boundary point on a smooth boundary .

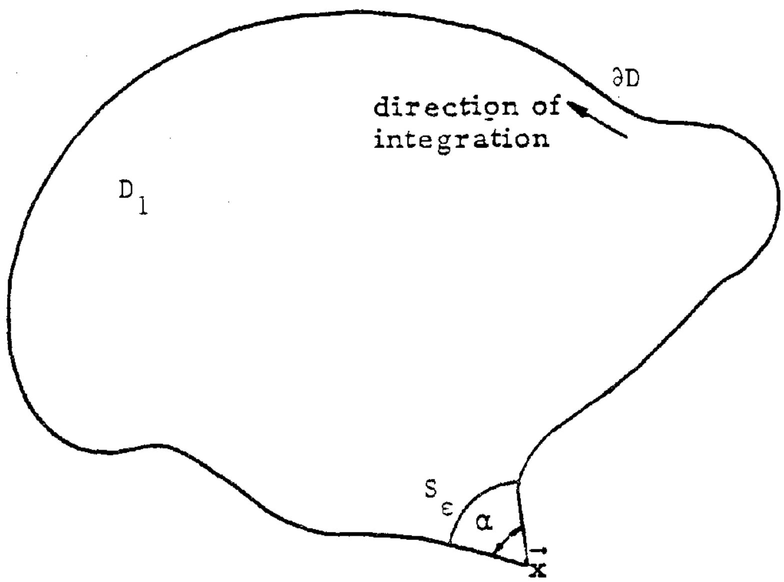

Figure A.3. Definition sketch for an interior point approaching a corner point on the boundary.